
SRF

# The Coaxial Blade Tuner – Final Report and Evaluation of Operation

A. Bosotti, C. Pagani, N. Panzeri, R. Paparella

INFN Milano, Lab. LASA,
Via Fratelli Cervi 201
Segrate (MI) - Italy

## Abstract

The future high gradient superconducting LINACS ask for the use of a compact and cost effective tuner design with no interference with the cavity end group area. The integration of the piezo-assisted fast tuning option made the Coaxial Blade-Tuner, an evolution of the device successfully tested at DESY on the superstructures, the most viable candidate to be included into the future LINACS BCD. The new tuner design is simpler and cheaper with respect to the former, still keeping the required mechanical stiffness. Actually, in the perspective of large scale production and on the basis of the experience acquired so far, two alternative prototypes have been designed and built. They mainly differ for the materials adopted (titanium or stainless steel) and have been optimized to minimize material and construction cost, while fulfilling the performances required for the high gradient cavity operation up to 35 MV/m or even higher.
The piezo blade tuner has been extensively and successfully tested both at room temperature and at cold once assembled on a TESLA type cavity in its final configuration. This report contains the full description of the device, starting from the mechanical features till the qualification test results inside the horizontal cryomodule facilities at DESY and at BESSY, showing the fulfillment of all the design requirements.

## Introduction – "Why a coaxial tuner design?"

The design of the TESLA cryomodule, since the release of TESLA TDR [1] in 2001, is driven by the request of a very high filling factor to reduce the accelerator length or to increase the effective accelerating field. One of the main improvements has been achieved in the interconnection between cavities. The TTF modules have installed cavities with a total length of 1384.8 mm, corresponding to a cell-to-cell distance of about 350 mm, exactly $3\lambda/2$ long. This length was actually chosen at the beginning of the linear collider studies only to obtain good cavity separation for the accelerating mode and simplicity in the phase adjustment. As a consequence, the effective accelerating gradient would be 17.8 MV/m only, in case cavities were operated at 25 MV/m. The fill factor, defined as cavity active length over cavity total length, has a low value of 0.75.

The main idea for the new tuner has been originally inspired by H. Kaiser [2] who studied a possible tuner solution for the *superstructure* option in TESLA [3]. This option is based on a different cavity chain layout, realized by means of non-resonantly coupled 7-cell cavities with shorter interconnection distance, corresponding to $\lambda/2$. This special design has been proposed in order to obtain a higher fill factor and simultaneously to increase the number of cells fed by a single input coupler.

The superstructure option has been later on discarded, but the search for a minimization of inter-cavity distance remained as the critical point to reduce the accelerator footprint. As a consequence, the present ILC reference layout [26], as well as for the TESLA design report before it, assumes a coaxial solution since the reduced total cell-to-cell space is incompatible with the current TTF tuner overall dimension.

Hence the development of a new frequency tuner able to guarantee the ILC cavity interconnection requirements has started. This new tuner [10] has been designed to be coaxial with the cavity and, by means of elongation of the helium vessel, to deform the cavity geometry and consequently change the resonance frequency. The tuner assembly is mainly composed of two parts, the movement leverage and the bending rings. The complete assembly of the tuner as mounted over the cavity helium vessel is shown in Fig. 1. The leverage system provides the amplification of the torque of the stepper motor, dramatically reducing the total movement and increasing the tuning sensitivity. A stepping motor, similar to those used for the TTF tuner, is rigidly connected to the helium vessel and produces a rotation of the big arm in the center of the tuner. The movement of the big arm induces the rotation of the bending system that changes the cavity length.

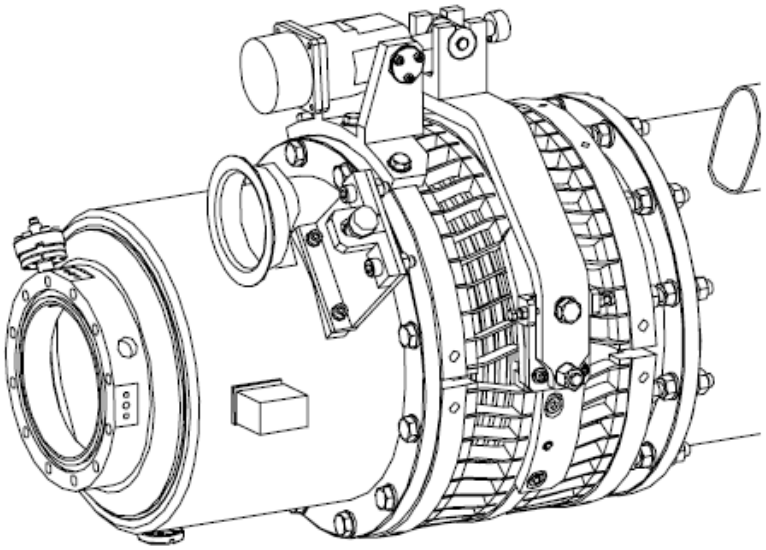

Fig. 1 – Drawing of the original Blade Tuner (SuTu tuner) assembly

The bending system consists of three different rings: the two external rings, which are rigidly connected to the helium tank, and the one at the center, symmetrically divided in two halves. The rings are connected by thin titanium plates, or *blades*, that can change the cavity length (compression and tension) as a result of an azimuthal rotation in opposite directions of the two halves of the center ring, through the bending of the blades. The big central arm is connected to the bending system to produce the rotation and the axial movement, which provides the cavity tuning.

This prototype model (named as original Blade Tuner or SuTu tuner, from the former SUperstructures TUner), successfully tested at DESY in 2002, both in CHECHIA and in the superstructures test module inserted in the TTF string [10][4][3], actually represents the reference design for the entire Blade Tuner activity, being the basis of the next models up to the present light and cheap device. One of the realized tuner prototypes, #IV or SuTu_IV, is shown in Fig. 2.

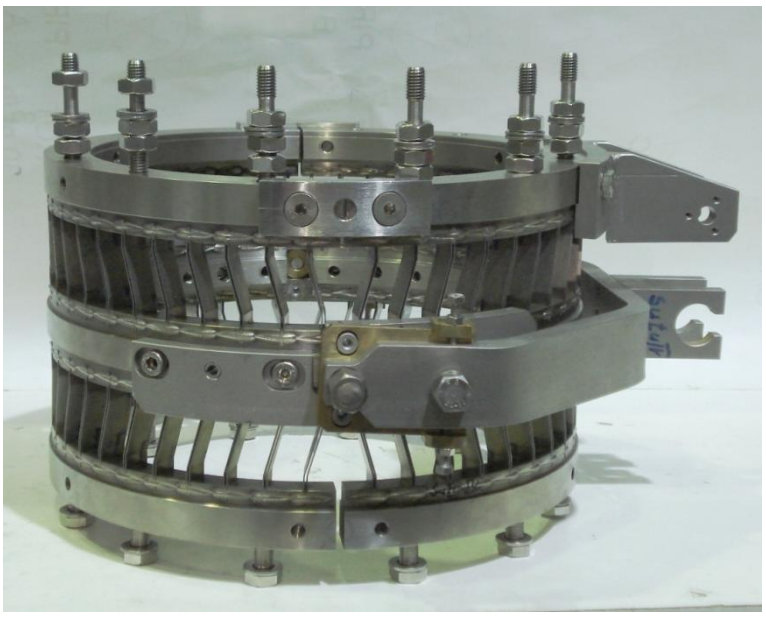

Fig. 2 –The SuTu_IV tuner

# 1. Blade Tuner Prototype

The working principle of the tuner is based on the bending of the blades that deform from the rest position (slant of 15° respect to the central axis) to a different configuration producing an elongation (or a shortening) of the tuner itself. This deformation is generated by the rotation of the central rings with respect to the lateral ones. In order to reduce the relative rotation of the lateral rings to nearly zero, and to balance the torsional moments, the central rings rotate in opposite directions and the blades are assembled symmetrically with respect to the horizontal plane. The rotation of the central rings is obtained through an outer leverage that is directly moved by the stepping motor and, through a connecting plate, induces a displacement in opposite directions of the edges of the central rings. A schematic representation of the kinematics of the tuner in its original design is provided in Fig. 3.

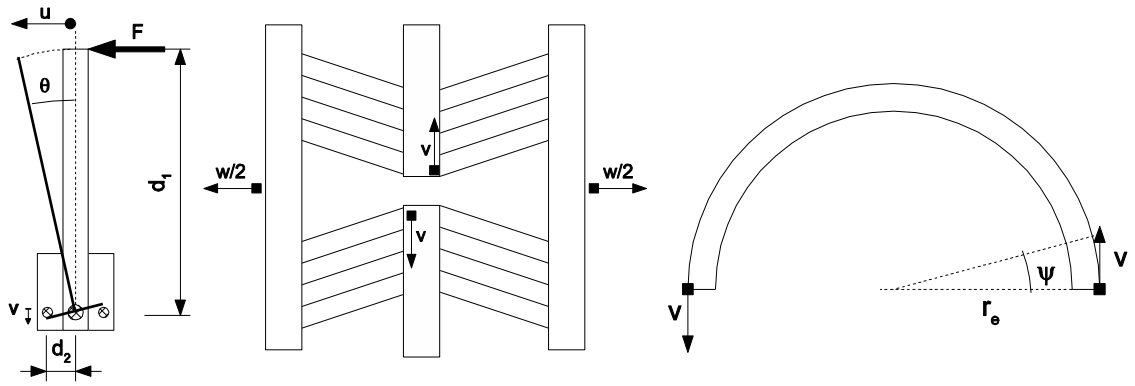


Fig. 3 - Cinematic description of the Blade Tuner tuning system

The mathematical relations among the involved variables are induced from simple geometrical considerations that are:

$$\theta = \arctan\frac{u}{d_1}$$

$$v = d_2 \tan\theta = u\frac{d_2}{d_1} \qquad (1)$$

$$\psi \cong \frac{v}{r_e} = \frac{u}{r_e}\frac{d_2}{d_1} = \theta\frac{d_2}{r_e}$$

# 2. Stiffness analysis and experimental results

The main composing parts of the assembly have been extensively reviewed in the previous tuner report [4]. Here we give emphasis to the first experimental compression tests on the prototype tuner at DESY, that will be eventually compared with the same quantities of the current blade tuner.

A prototype of the bending system has been fixed on a accurate measuring machine while the central ring was rigidly fixed by means of two proper mechanical fixtures to avoid internal rotation (in this configuration, due to the symmetry of the inner ring, the tuner is in the same configuration of the operative one, simulating a leverage system with infinite stiffening). The same measurements have been repeated with the leverage mechanism to check its influence too. The structure has been compressed along the axes with different loads while monitoring,

with a micrometric LVDT sensor[1], the deformation of the mechanism. Pictures of the experimental setup are reported in Fig. 4. The results of these tests are summarized in Tab. 1, compared with the results of some 3D FEM simulations [5], where possible. A simplified 2D (single blade) analysis in the load cases #2 and #3 are also presented in Table 1 for sake of completeness.


Fig. 4: Pictures of experimental compression tests on blade tuner, showing both the experimental configurations.

| **Boundary conditions for the central tuner ring** | | **Experimental** kN/mm | **2D model** kN/mm | **3D model** kN/mm |
|---|---|---|---|---|
| No rotation – links installed<br>Translation allowed in axial direction<br>Fx = 0; $\psi_{LC} = 0$ | | 83.3 | --- | 120.2 |
| No rotation<br>No translation<br>$u_{LC} = 0$; $\psi_{LC} = 0$ | load case 2 | --- | 155 | 164.2 |
| Free | load case 3 | --- | 2.5 | 3.2 |
| **Leverage mechanism installed – real case** | | **25** | --- | 83.7 |

Table 1 – Blade Tuner axial stiffness values for different boundary conditions

[1] Linear Variable Differential Transformers (LVDT) are a class of electrical transformers used for measuring linear displacements. A cylindrical ferromagnetic core, attached to the object whose position is to be measured, slides along the axis of three solenoidal coils [139].

From the comparison between experimental and simulated data, it comes out that the final stiffness value expected from the 3D FEM analysis of the tuner in its real working setup (i.e. leverage mechanism installed) is closer to the experimental result of the first case, rather than the nominal one. This means that the leverage and motor assembly is not an ideal and infinitely rigid boundary for the central ring of the tuner (as one is forced to consider in the FEM analysis), as is instead the case for the stainless steel links considered for the first case. For these reasons, the measured value of 25 kN/mm, will be considered further on as the reference stiffness value of the Blade Tuner prototype.

# 3. Modified Helium Tank

The cavity helium tank (He tank) has to allow the elongation required by the installed tuning mechanism in order to change cavity frequency. In the case of the coaxial Blade Tuner, a modified helium tank has been designed and realized installing a bellow in the middle of the tank, thus permitting the coaxial operation of the tuner. bellow the tuner rings as shown in Fig. 5 and Fig. 6.

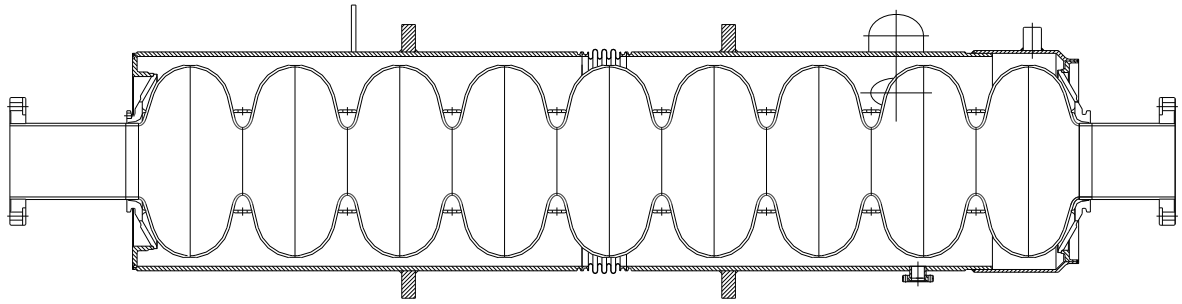

Fig. 5 – Drawing of the cross section for the cavity assembly with the modified He tank

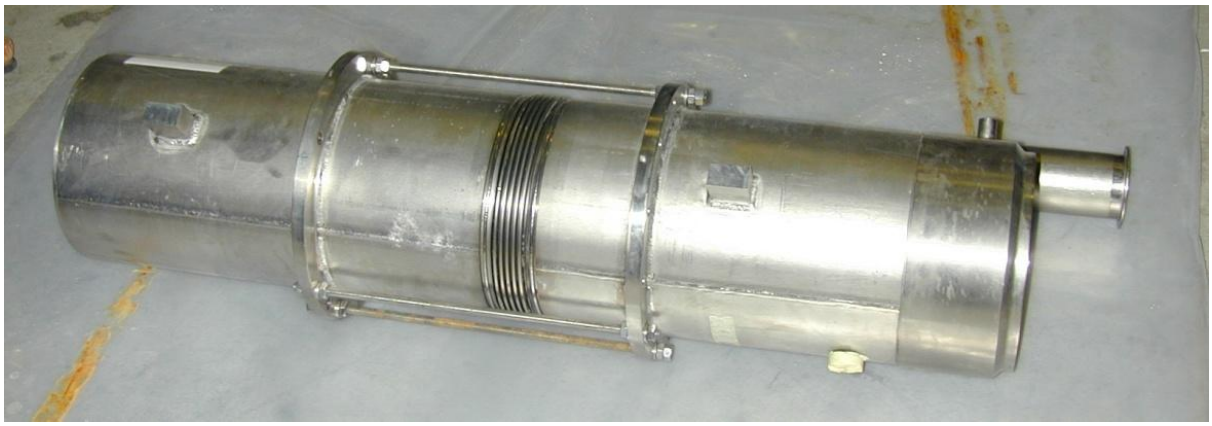

Fig. 6 – The modified He tank. The support screw rods, visible between welded rings, are temporarily placed to save the bellow from unwanted deformations.

In order to evaluate the final longitudinal stiffness for this He tank revised design, FEM analyses have been performed separately for both the vessel, considered as one single part of 1007 mm length, and the bellow. Similarly to every stiffness evaluation through a FE model, resulting value has been obtained imposing a longitudinal displacement of 1 mm at one side and computing the reaction force at the same point. Results for the helium vessel components are $k_H$ = 302.4 kN/mm and $k_B$ = 0.19 kN/mm longitudinal stiffness for the vessel and the bellow respectively. In these cases, FEM analyses were conducted on a 2D model of the element.

An essential role for what concerns the overall longitudinal stiffness of the assembly is played by the two rings that connect the vessel to the cavity, usually named as end dishes or washer disks. For the modified Blade Tuner He tank, the end dishes have been adapted from the original TTF design without any optimization. The ANSYS 2D finite element model of the end dish at the coupler side is reported in Fig. 7 a.

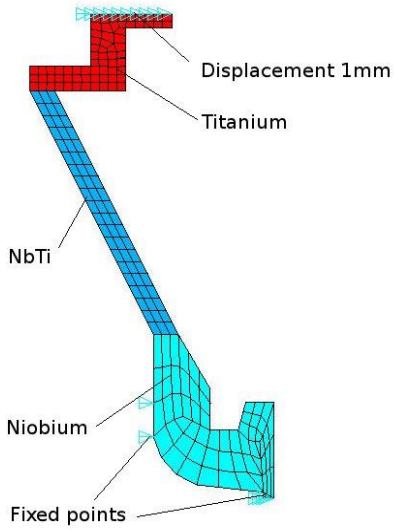


Fig. 7.a - End dish coupler side model

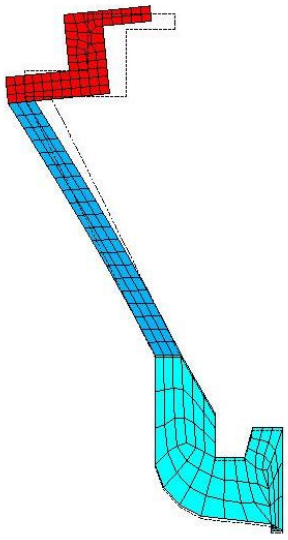

Fig. 7.b – End dish coupler side deformed

By imposing a displacement of 1 mm at the washer disk connection ring upper face, the structure reacts with a force that corresponds to an equivalent stiffness $k_W^C$ of 24.8 kN/mm. The displacement obtained is shown in Fig. 7 b. A similar analysis, carried out on the end dish at the opposite side, or tuner side, that has a different design, reveled a higher stiffness value $k_W^T$ of 32.2 kN/mm. These two results allowed to estimate the overall longitudinal stiffness $k_W$ of the whole assembly composed by the series of both end dishes. Therefore:

$$k_W = \frac{k_W^C \cdot k_W^T}{k_W^C + k_W^T} = 14 \ {}^{kN}/_{mm}$$

In order to check that the vertical displacements of the cavity, when it is installed in a modified He tank with central bellow and coaxial tuner, are compatible with the required alignment precision of 0.5 mm for the cold mass string, some axis-symmetric analyses with non axis-symmetric load have been also performed [4]. The used FEM model replicates the bending due to all dead loads in the system without accounting for additional external solicitations. The coaxial tuner is considered only as a load and the stiffening effect of the four threaded bars is not considered.

Resuming results, analysis reveals that the total dead load (cavity plus helium tank and piezo Blade Tuner) is 598 N and the maximum vertical deflection of the cavity with respect to its ends is of 0.115 + 0.144 = 0.259 mm, lower than the specifications required for the alignment of the cells. Finally, also the tensile stress on the bellow has been analyzed. Neglecting the stress concentrations near the welding point, that are not accurately meshed, the maximum stress in the bellow is equal to 6.3 MPa, lower than the admissible value given by the manufacturer.

# 4. Piezoelectric actuators integration

Piezo-ceramics actuators (piezo) are used to provide fast tuning capability to the blade tuner. The piezoelectric option for LFD compensation needs have been now widely validated thanks to several successful tests performed with the TTF fast tuner [9][12][14][19]. To be efficient and flexible, the active elements integration must follow some guidelines, such as

- Commercial but affordable piezo elements as the first choice for actuators.
- Flexible actuator accommodation, in order to preserve the possibility to install piezo of different sizes or even completely different solutions ( e.g. magnetostrictive etc. [27]).
- Ensure slow tuner efficiency even against an eventual complete failure of fast actuators.
- Keep the overall design as simple as possible to reduce the number of additional elements compared to the existing Blade Tuner and lower costs.
- Provide a high axial stiffness for the final assembly in order to lower the sensitivity to Lorentz force detuning and easing fast actuators requirements.

The detailed results obtained by the FEM analyses of the Blade Tuner and its components, discussed in previous paragraphs and which provided accurate information on stresses, deformations and stiffness, have been also used for the integration of the fast tuning elements. Piezoelectric actuators, that represent the reference choice, are subject to several requirements limiting the possible design configurations. First of all, the piezoelectric actuators cannot be subject to tension forces, and bending and shear actions need to be carefully avoided. Moreover, in order to maximize their lifetime, a correct preload range needs to be guaranteed under all operating condition [6]. In addition to that, the characteristic behavior of piezo operation at cryogenic temperatures, in terms of stroke and preload effects, has undergone a systematic investigation [7].

Finally, referring to the typical values of the TESLA type structures in terms of cavity elasticity and tuning requirements [7], piezoelectric elements have been integrated by inserting two elements between one of the end rings and the corresponding flange on the He vessel, as shown in Fig. 8 and Fig. 9 where He tank and cavity are not shown for simplicity. The different tuner parts in these pictures are color-coded by material type: blue denotes Ti, gray stainless steel, yellow CuBe and red brass. The piezo elements are the dark gray rectangular bars acting on the left Ti ring.

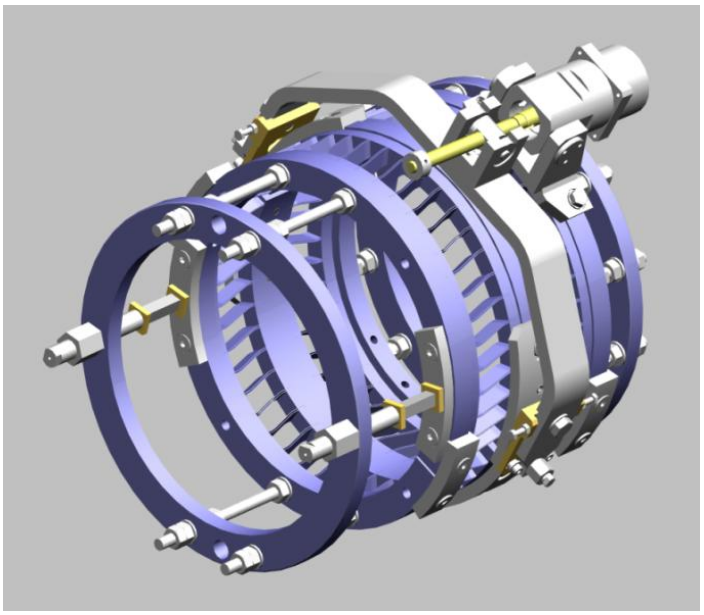

Fig. 8 – The Blade Tuner design after piezo actuators integration

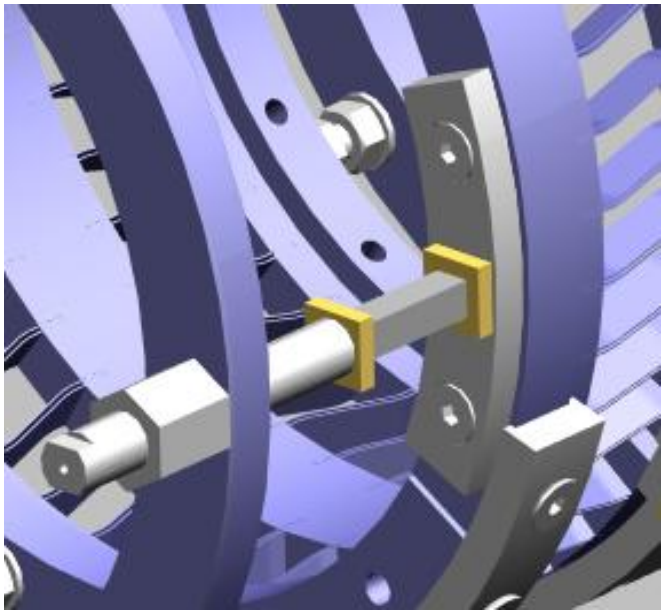

Fig. 9 – Detailed view of piezo integration in the Blade Tuner

The main idea below this design choice has been to allow the cavity itself, through its axial stiffness, to generate the mechanical preload needed by the piezo actuators [23]. A cavity pre-tuning procedure has been developed in order to guarantee the correct range of preload values on the piezoelectric elements along the entire slow tuning range. This procedure allows also avoiding the "neutral" point of the leverage system and requires that the tuner operation always acts stretching the cavity, thus compressing the piezoelectric elements.

The position of the piezo actuators has been carefully chosen in order to avoid possible stresses due to the deflection and vibration of the helium tank. The active elements are kept in position by means of supports as shown in Fig. 9: they can accommodate elements of length up to 72 mm and a spherical head can be used in order to minimize shear and bending forces.

In addition to the piezos, four threaded bars have been introduced on the upper and lower side of the assembly (see Fig. 10). These bars, parallel to the piezo elements accomplish two different tasks. First of all they are needed during transportation, handling and assembly

phases to avoid plastic deformations of the bellow. In this case they are tightly bolted at both ends to provide stiffness to the system. Furthermore, in operating conditions, the inner bolts are loosened by a calibrated distance (less than one mm) and the bars act as safety devices in case of piezo mechanical failure or overpressure conditions inside the helium tank. With respect to the original system used for the TTF superstructures, the leverage system has been rotated to one side, in order to avoid the mechanical interferences with the Invar rod providing the cavity longitudinal alignment in the TTF CRY3 design. The overall final assembly is shown in Fig. 10

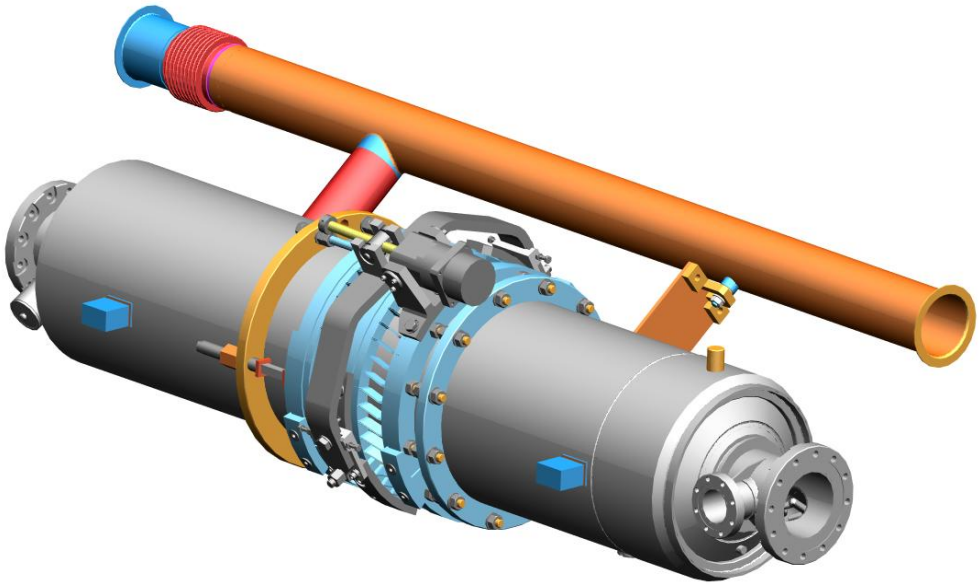

Fig. 10 - The cavity dressed with the modified helium tank and piezo Blade Tuner.

The choice of the reference piezo actuator to be installed in the Blade Tuner took advantage of the R&D activity on commercial piezoelectric actuators [4], and of the latest results concerning LFD compensation performances [12][19]. Finally, two complete Blade Tuner assemblies with corresponding modified He tank have been manufactured and equipped in order to include the piezo active elements. For these first assemblies, 40 mm length piezo actuators from NOLIAC (NOLIAC_40) has been chosen for installation. Properties of interest for this piezo model are reported in Table 2

| Parameter | Requirements room T | Dimensions |
|---|---|---|
| Max stroke - $L_{max}$ | > 40 | µm |
| Blocking force - BF | > 4 | kN |
| Stiffness - $K_P$ | >> 3 | kN/mm |
| Load limit - LL | > 10 | kN |
| Res. freq | > 10 | kHz |
| Life-time | > 10^9 | # cycles |
| Act. Voltage | ≤ 200 | V |
| Size | 20 x 20 x 100 | $mm^3$ |

Table 2 – Piezo specifications for the fast frequency tuning

# 5. Cavity Equipped with Helium Tank and piezo blade tuner

The behavior of the cavity when equipped with helium tank and tuning system can be now finally analyzed, since it strongly depends from the stiffness of each component. In this paragraph axial and bending models are developed taking into account all the stiffness values obtained through analyses and simulations reported before. This model of the whole assembly is needed to evaluate the requirements for the piezo actuators and to check that the cavity external stiffness approaches the hypothetical value of 30 kN/mm (as desired from the $K_L$' Lorentz coefficient analysis, see for example refs [4] and [12]). Moreover this analytical approach can be applied also to different tuner models.

Firstly, the mechanical characteristics of all involved parts at room temperature are reported in Table 3. The following analytical models and corresponding computations are strictly valid for the system at room temperature (RT), even if results are considered as valid also for the nominal working conditions at 2 K. This assumption is justified by the fact that it is expected that the stiffness of the core spring element in the system, the cavity, is not varying significantly from RT to 2 K temperature. In addition to this, the effect of temperature lowering on all the other components, from end dishes to tuner, generally leads to an increasing of the stiffness of each component. So, the assumption to keep RT values for system modeling can be considered as the choice to face the worst case for the system. Finally recent further FEM simulations performed at the FNAL laboratory seem to confirm the former assumption about the longitudinal stiffness increasing of the cavity, from 300 to 2 K, is expected to be limited to 10 % [15].

| Part | Material | Axial stiffness | c (mm/kN) | k (kN/mm) | Notes |
|---|---|---|---|---|---|
| Helium tank | Ti Gr2 | $k_H$ | 3.30 | 302.4 | |
| Blade Tuner | Ti Gr2 | $k_T$ | 40.0 | 25 | From exp. |
| Cavity | Nb | $k_C$ | 330.8 | 3.023 | |
| Washer disk | NbTi | $k_W$ | 71.4 | 14 | Both disks |
| Piezo actuator | PIC 255 | $k_P$ | 4.46 | 2 x 112 | |
| Tuner bellow | Ti Gr1 | $k_B$ | 5263 | 0.19 | |

Table 3 - Mechanical characteristics Blade Tuner components RT

The analysis starting point is an axial model with associated displacements and forces, both for slow and fast tuning actions.

In the slow tuning phase the stepper motor applies a deformation to the blades in order to tune the cavity to the right frequency. It is supposed that the Blade Tuner applies a displacement $\delta_t$ to the system: with this assumption the cavity will be stretched and the helium tank compressed. Globally the system remains in equilibrium and the axial stiffness model is shown in Fig. 11.

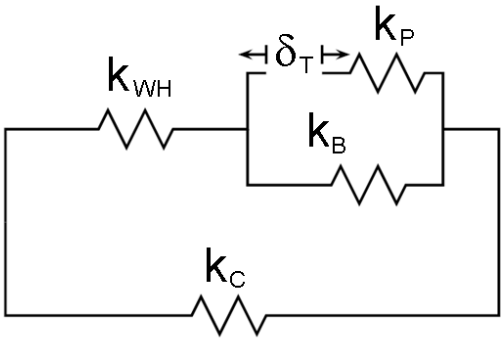


Fig. 11 - Axial model for the slow tuning action of the Blade Tuner assembly

From simple considerations the expression of the total stiffness $k_{WH}$ of the series composed by helium tank and both end dishes is:

$$k_{WH} = \frac{k_W k_H}{k_W + k_H} = 13.38 \text{ kN/mm}$$

Then, from equilibrium and congruence:

$$\begin{cases} \delta_C = \delta_T + \delta_{WH} + \delta_P \\ \delta_B = \delta_T + \delta_P \\ F_C = k_C \delta_C \\ F_{WH} = k_{WH} \delta_{WH} \\ F_P = k_P \delta_P \\ F_B = k_B \delta_B \\ F_{WH} = -F_C \\ F_{WH} = F_B + F_P \end{cases}$$

Solving the consistent equations it is possible to obtain the displacement of any part as a function of the tuner displacement:

$$
\begin{cases}
\Delta = k_p k_{WH} + k_B (k_C + k_{WH}) + k_C (k_p + k_{WH}) \\
F_{p=} - \dfrac{k_p [k_C k_{WH} + k_B (k_C + k_{WH})]}{\Delta} \delta_T \\
F_B = \dfrac{k_p k_B (k_C + k_{WH})}{\Delta} \delta_T \\
F_{WH} = - \dfrac{k_p k_C k_{WH}}{\Delta} \delta_T \\
F_C = \dfrac{k_p k_C k_{WH}}{\Delta} \delta_T \\
\delta_p = - \dfrac{k_C k_{WH} + k_B (k_C + k_{WH})}{\Delta} \delta_T \\
\delta_B = \dfrac{k_p (k_C + k_{WH})}{\Delta} \delta_T \\
\delta_{WH} = - \dfrac{k_p k_C}{\Delta} \delta_T \\
\delta_C = \dfrac{k_p k_{WH}}{\Delta} \delta_T
\end{cases}
$$

Finally, the axial force that every part has to withstand as a response to a tuner displacement of 1 mm is reported in Table 4, while the displacements are reported in Table 5.

| Part | Force for a $\delta_t$ = 1 mm (kN) |
|---|---|
| Helium tank / End dishes | -2.435 |
| Blade Tuner | -2.623 |
| Cavity | 2.435 |
| Piezo actuators (total force) | -2.623 |
| Tuner bellow | 0.188 |

Table 4 - Axial forces for a tuner displacement of 1 mm. Tensile forces are positive

| Part | Displacement for a $\delta_t$ = 1 mm (mm) |
|---|---|
| Helium tank / End dishes | -0.182 |
| Blade Tuner | 1 |
| Cavity | 0.806 |
| Piezo actuators | -0.013 |
| Tuner bellow | 0.988 |

Table 5 - Axial displacements for a tuner displacement of 1 mm. Elongations are positive

In the fast tuning phase the piezoelectric actuators displacements are in the order of some microns in order to contrast the Lorentz force detuning. It is supposed that both the piezo actuators in parallel apply a displacement $\delta_p$ to the system, with the assumption that the cavity is stretched and the helium tank compressed. Neglecting the dynamic effects, the resulting axial stiffness model is shown in Fig. 12.

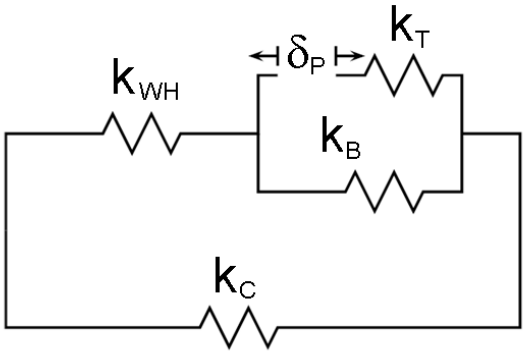


Fig. 12 - Axial model for the fast tuning action of the Blade Tuner assembly

Following the same analytical procedure of the previous case, making the $\delta_t$ in $\delta_p$ and $k_p$ in $k_t$ substitutions, results can be found from equilibrium and congruence and then solving the consistent equation. The axial force that every part has to withstand for a piezo displacement of 1 μm is reported in Table 6, while the displacements are reported in Table 7.

| Part | Force for a $\delta_p$ = 1 μm (N) |
|---|---|
| Helium tank / End dishes | -2.229 |
| Blade Tuner | -2.401 |
| Cavity | 2.229 |
| Piezo actuators (total force) | -2.401 |
| Tuner bellow | 0.172 |

Table 6 - Axial forces for a piezo actuators displacement of 1 μm. Tensile forces are positive

| Part | Displacement for a $\delta_p$ = 1 μm (μm) |
|---|---|
| Helium tank / End dishes | -0.167 |
| Blade Tuner | -0.096 |
| Cavity | 0.737 |
| Piezo actuators | 1 |
| Tuner bellow | 0.904 |

Table 7 - Axial displacements for a piezo actuators displacement of 1 μm. Elongations are positive

Finally, the performed analyses showed that the actual efficiency of the slow tuning action for the Blade Tuner can be estimated in 80.5 % while it is 73.7 % for the fast tuning action. These results specify the amount of piezo stroke to be guaranteed for them to be useful for the LFD compensation purposes. Anyway, the 40 mm long piezo stacks from NOLIAC (NOLIAC_40) that have been chosen as a starting reference design ensure sufficient stroke margin at cold. Moreover an even safer solution, in terms of performances margin, has been considered and it is based on even longer piezo stacks, 70 mm long and 15 x 15 mm cross section from NOLIAC (NOLIAC_70, see Table 19 in the APPENDIX and ref. [11]).

The presented model for the complete cavity system is then also useful to evaluate the cavity external stiffness. According to the schematic representation in Fig. 12, the $k_{ext}$ value can be simply obtained computing the equivalent total stiffness for the upper section of the scheme including end dishes, bellow, piezo and tuner. The resulting value is $k_{ext}$ = 8.3 kN/mm, therefore significantly lower than the goal value of 30 kN/mm mentioned before. It is anyway clear from the mechanical analyses performed, see results in Table 4 and

Table 6, that the actual main stiffness loss, as well as the main tuner displacing action loss, are located in the cavity end dishes, that are the softer elements in the whole cavity constraining assembly. This limiting effect is preserved also if, for instance, the stiffness of the tuner mechanism is raised, as visible in Fig. 13 where the resulting $k_{ext}$ is plotted as a function of the $k_T$ according to the current system configuration.

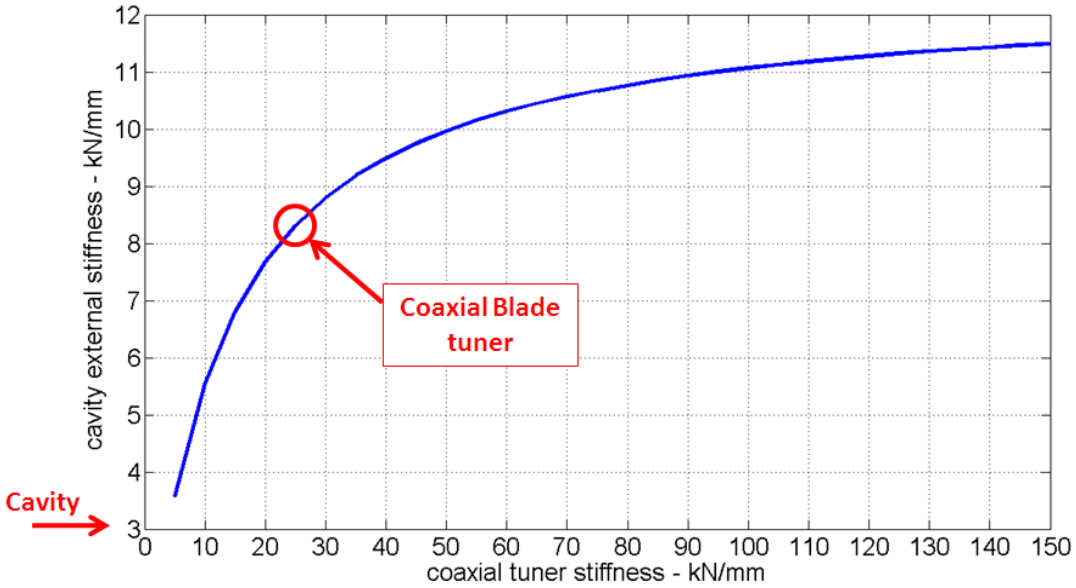


Fig. 13 – Cavity external stiffness as a function of coaxial tuner stiffness, the current design of the modified He tank and end dishes is assumed

So, even if some limited improvement is possible, analysis confirms that it is not possible to reach an optimum external stiffness value with the current end dish configurations for the coaxial tuner. The role of the end dishes therefore becomes critical, especially in the case of a coaxial tuner, when the tuning displacement is transferred to cavity through both of them.

As reference, considering for instance the TTF tuner assembly instead of the coaxial one but installed on the same system configuration, the proposed spring model can be used with the assumption that only the coupler side end dish contributes to the $k_{WH}$ value. So, for a $k_{WH}$ of 22.9 kN/mm the $k_{ext}$ results to be about 16 kN/mm. So, although the estimated external stiffness for the TTF tuner case is almost two times higher than the coaxial tuner case one, the actual improvement in term of dynamic Lorentz coefficient is lower as can be inferred by the plot in Fig. 14, where results from $K_L$ analysis have been used [12].

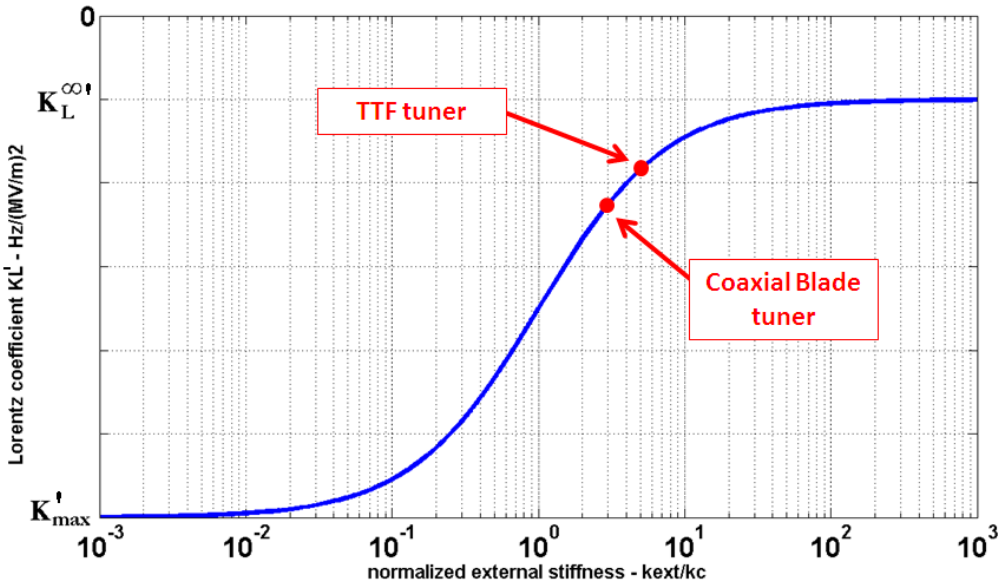


Fig. 14 – LFD coefficient as a function of the normalized external stiffness for both the TTF and coaxial tuner solutions

Therefore, it is possible to expect for the coaxial tuner solution to lead to a higher sensitivity to Lorentz force detuning but, in parallel, to ensure an higher fast tuning efficiency than the TTF original solution, that is limited by the same leverage geometry itself.

In conclusion, it is clear that in any case the current helium tank end dish design must be revised in order to reach higher stiffness for the cavity constraining mechanism and to increase tuning efficiency. Therefore, in parallel to the development of the coaxial tuner itself in view of large scale production and costs reduction, the study of a new end dishes design is ongoing. The main result in the frame of the former activity has been the realization and the test of renewed design model for the Blade Tuner. Details on this will be presented in following paragraphs.

# 6. The new blade tuner design

Since 2003, an activity is ongoing mainly focused on the redesign of the Blade Tuner in view of the long term feasibility of the ILC proposal [26]. For the ILC project more than 16000 coaxial tuner are required. The effort to optimize its design is widely justified by the subsequent enormous cost saving. Moreover the actual blade tuner version, although proved to fulfill the slow tuning requirements , it is far from being in the final design stage and some modifications are required in order to improve its reliability and reduce its total cost.

Two aspects have been considered in the optimization process here presented: first of all a global design refinement of rings and blades has been performed. This has been obtained taking into account both the geometry and the material of the blade tuner, allowing developing a unique geometrical solution that can be realized with the rings in titanium or stainless steel. This is very important in view of a possible future use of a steel helium tank when the technology will allow solving the problems in welding titanium to stainless steel. The second aspect considered concerns a major simplification of the driving mechanism and the moving of the motor from a central to a lateral position. The effectiveness of this solution has been proved by means of experimental tests and numerical simulations.

The original Blade Tuner as it is shown in Fig. 1 has been the starting point of this activity and it allowed several improvements. The whole weight of the original mechanism is approximately 20.5 kg. Each half blade-ring assembly has an array of 23 “packs” of 2 blades on

each side, for a total of 184 blades. The blade packs for the two halves of the blade-ring assembly are electron-beam welded in a single pass with a special tooling device, in order to limit any unnecessary loading/unloading procedures of the electron beam welding machine, which leads to an increase in costs and to longer manufacturing times

## 6.1. A slimmer and cheaper design

On this base, exploration of possible simplifications and cost reduction efforts for an industrial scale Blade Tuner began. Titanium has been chosen as the reference tuner material in the early stage of the design development activity. As for the original Blade Tuner model, this choice grants both thermal shrinkage compatibilities with the materials used for the helium tank and cavity (respectively, Ti and Nb), and good elastic and strength properties, which allow to reduce the stresses in the flexural elements. Later on cheaper structural materials options, as stainless steel, have been considered.

First of all, a conceptual preliminary design has been presented [16][18]. By lowering the requirements on the ring-blade stiffness a first "lighter" version was devised, which reduces the needed material and the number of machining and weld procedures. A preliminary result of this study is shown in Fig. 15, using the same material color coding used for previous Fig. 8.

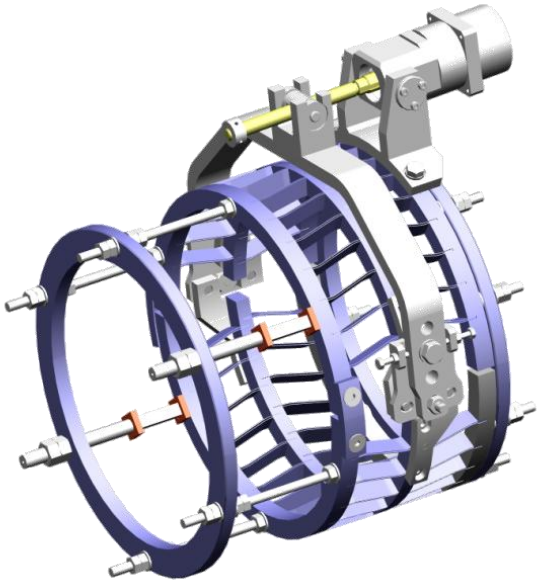

Fig. 15 – Prototype revision of a lighter Blade Tuner

The width of the Ti rings has been reduced, as well as the number of blade elements. Now the system has an array of 14 "packs" of 2 blades on each side, for a total of 112 blades, with a 40% reduction in the number of blade packs, and a consequent reduction of the assembling time and number of EBW welds. This leads to a corresponding decrease of the nominal stiffness of the ring-blade mechanism that is anyway consistent with the overall stiffness requirement dominated by the other system components, mainly by the helium tank end dishes. Fig. 16 shows the details of the blade packing into the tuner rings in the two designs.

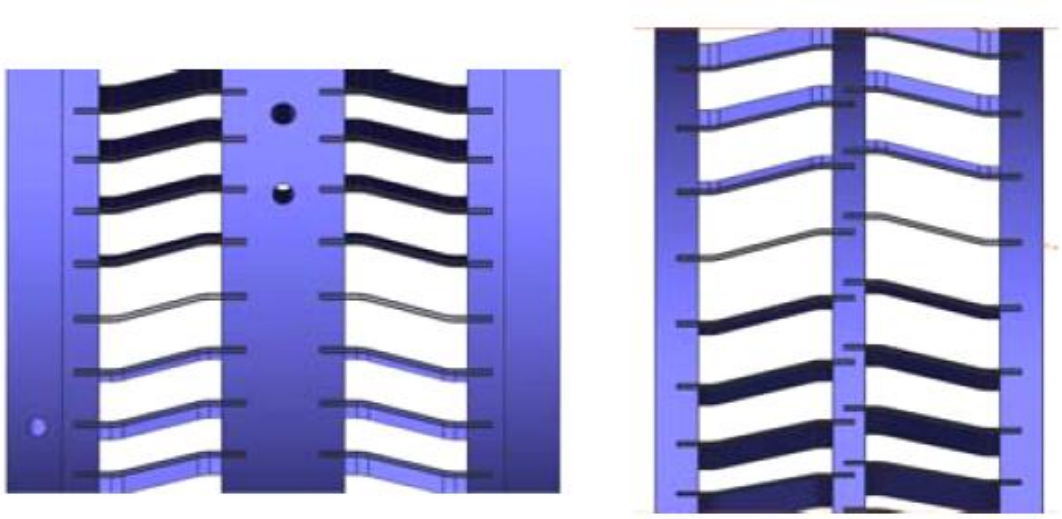

Fig. 16 – comparison between the original design (left) and the lighter prototype (right)

In this case the blade position at the central ring is no longer collinear on the two opposing sides, but is assembled in an alternated pattern, allowing welding the two opposite blade packs in a single electron beam welding (EBW) seam. The total weight of the tuner is now slightly less than 12 kg, thus allowing a direct 40% decrease in Ti material costs.

For this first concept of revised coaxial tuner, an important modification has been introduced concerning the design of the blades themselves since length and width have been adjusted so to significantly improve the tuning range. The new design makes use of longer blades as reported in Table 8 (see [4] for a reference blade scheme). This allows increasing the displacement induced on the cavity to 1.5 mm instead of 1.1 mm as for the original design.

| **geometry** | **Material** | **blHor** mm | **blCla** mm | **blVer** mm | **blLen** mm | **blRad** mm | **blWid** mm | **blThi** mm |
|---|---|---|---|---|---|---|---|---|
| original | Ti gr.5 | 12 | 8 | 7.5 | 56 | 15 | 15 | 0.5 |
| new | Ti gr.5 | 12 | 8 | **10** | **66** | 15 | **16** | 0.5 |

Table 8 – Blades dimensions for the revised Blade Tuner design

Several FEM analyses have been performed also on this blade design in order to fully characterize the behavior in terms of load limits and stiffness. Two main issues are considered as limiting the compressive load on the blades. Firstly, buckling is a typical failure mode that is addressed for slender elements like tuner blades, it is related to both material used and shape. It is characterized by a sudden failure when the object is subjected to a compressive force and an equilibrium configuration different from the original exists. This occurs at stress level lower than the ultimate compressive stresses that the material is capable of withstanding. Therefore a safe and lower load limit must be ensured for the single blade as well for the whole tuner. Moreover internal mechanical stresses in the blade are evaluated through the von Mises criteria [17]. This is widely in use to predict failure by ductile tearing or plastic strains in materials like metals, arising when the corresponding stress limit, given for every material, is locally overcome. As a reference, both internal stresses and the axial load vs. displacement curve are presented in Fig. 17 and Fig. 18 respectively for the blade at its the maximum admissible deformation, that has been assumed equal to 70% of blVer (see Table 8).

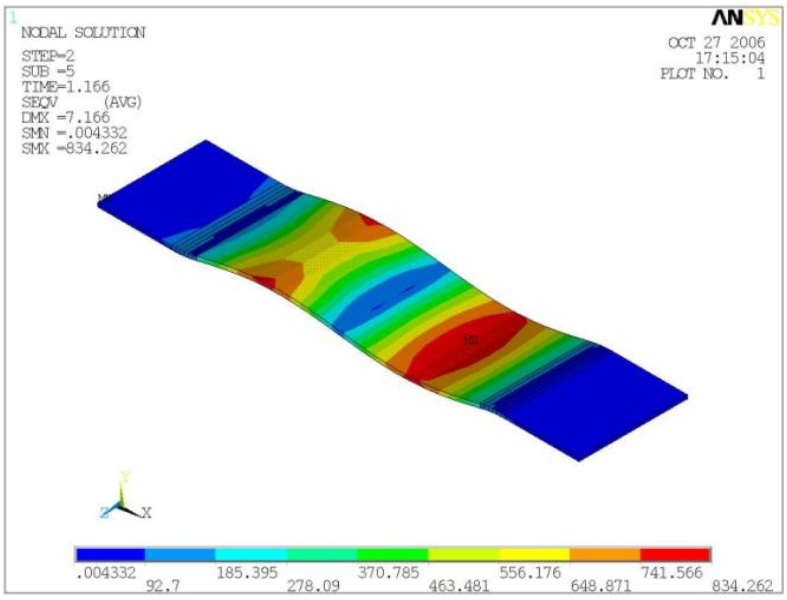


Fig. 17 - Von Mises stresses on blade after the application of an axial load at the maximum admissible deformation

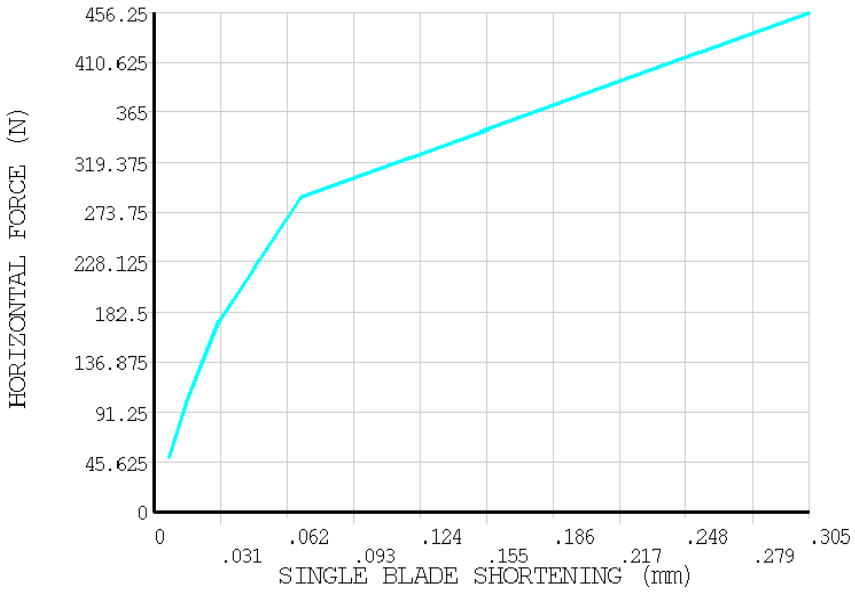


Fig. 18 – axial load vs. displacement for the maximum deformation configuration

Analysis allowed estimating the stiffness and the main load limits for the new blade design and to compare it to the original one. The final results are reported in Table 9.

| geometry | Material | Limit load stressed state | Max load before plastic strains | Limit load non stressed | Buckling load non deformed state | Limit load final | Stiffness | Tuning range cavity disp. |
|---|---|---|---|---|---|---|---|---|
| | | N | N | N | N | N | kN/mm | mm |
| Original | Ti – gr2 | 786 | 709 | 669 | 427 | 223 | 6.49 | 1.1 |
| New | Ti – gr2 | 486 | 456 | 496 | 290 | 162 | 5.43 | 1.5 |

Table 9 – Summary of FEM analyses for a single blade with revised design.

This information finally lead to the correct choice of the blade distribution along the tuner circumference, always keeping as a reference the main guidelines of simplification and welds reduction previously introduced. Because the final cost will depend from the numbers of machining operations, a total number of 96 blades are used. They are grouped in 6 packs of 4 blades each for each half ring collinearly welded on the central ring, thus allowing a 75% reduction of welds and a simplification of machining operations with respect to the original configuration. This will simplify the machining operations without a noticeable weight increase. In parallel to the development of the design of the tuner blade assembly, a key improvement has been also introduced concerning the former leverage mechanism of the Blade Tuner. The original driving system is composed of a stepper motor that, by means of a leverage arm, moves the two central rings pulling one side and pushing the other one such to have a perfect symmetric system. This solution, although it ensures high tuning sensitivity and a perfect symmetrical behavior, is cumbersome and expensive. In particular the friction between rotating and translating parts makes them a weak point that has to be solved in a radically way in order to reduce non-linearity. Therefore a simplified driving system has been realized, reducing drastically the number and complexity of parts.

Finally, the revised design solution, with the chosen configuration of the new Blade Tuner rings and blades is presented in Fig. 19. The simplified driving system is also visible, mainly composed by the motor with its harmonic drive and a CuBe screw. The axial movement of the nut is directly transferred in the rotational one by the central rings.

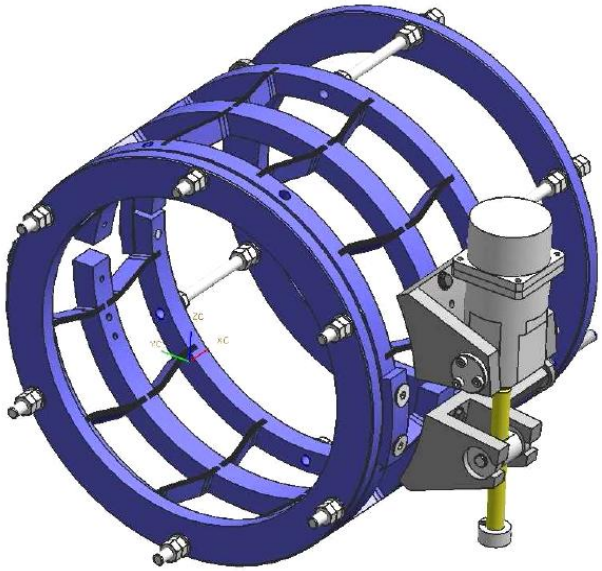

Fig. 19 – the new design of the Blade Tuner with the revised driving system

Although this arrangement simply push away the two central rings at one side, therefore losing the complete symmetry, finite element computations and experimental test proved the effectiveness of the solution. The experimental test was performed at LASA laboratory by using a simplified mechanism in substitution of the motor. The displacements recorded at the free rings showed a correct axial movement with negligible rotational or translation effects. This result has also been confirmed by FEM computations performed on the new tuner geometry. In particular Fig. 20 shows the axial displacements at the maximum possible deformations blades, corresponding to the tuner longitudinally expanded up to its maximum position.

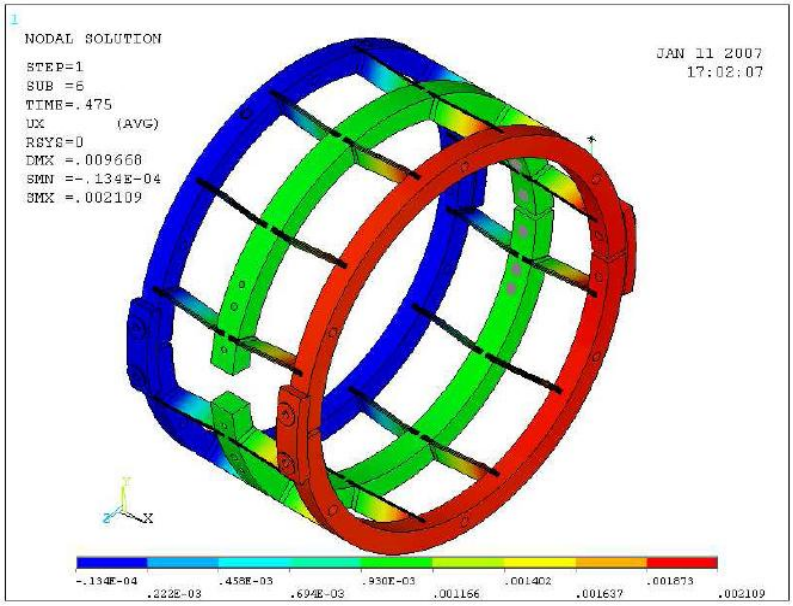


Fig. 20 – Computed axial displacements for revised Blade Tuner design with lateral motor

The maximum axial force on the motor in this configuration, evaluated in 400 N is fully compatible with the motor and harmonic drive currently used. The only apparent drawback of the new design is the lowering, due to the lack of the de-multiplication factor of the leverage, in the tuning sensitivity by a factor of about 7. Nevertheless the value corresponding to the proposed configuration, that can be expected to be at most up to 3 Hz per motor step, can be considered as consistent with the experience gained with TTF/FLASH operations.

The modifications presented for the Blade Tuner and based on the new blades shape and distribution, lighter rings and lateral motor without leverage, have been summed up in a new proposal design, slimmer and cheaper in comparison to the original design.

The use of a coaxial tuner opens different possibilities to optimize the geometry of the helium tank and of the cavity end group. In particular the revised tuner design presented is lighter and more compact than the previous one. Positive consequences are a lower impact on the deflection of the cavity and a larger free space for the positioning of the cryomodule elements such as the invar rod. All this has been obtained maintaining the compatibility with the older design, so that this new version can be installed in the already made helium tank only by means of simple adapters. A comparison of the old and new tuner design is shown in Fig. 21. It is clear that the space in the upper part of the helium tank is almost all free, giving an easy access to the positioning of the invar rod.

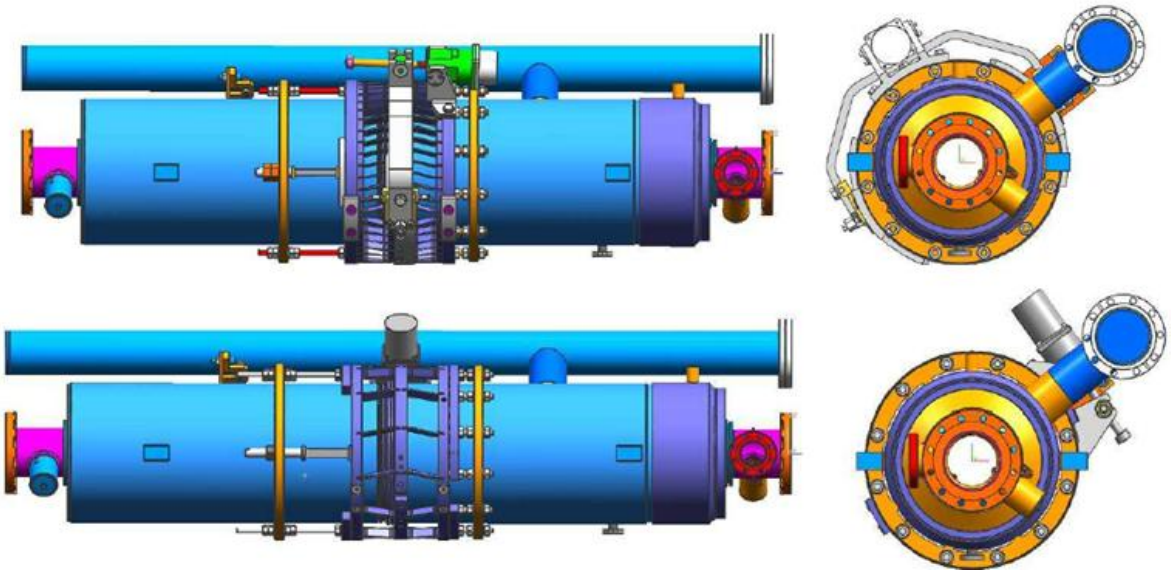

Fig. 21 – Original and revised design Blade Tuners installed on a modified He tank, lateral (left) and frontal (right) views.

## 6.2. Materials and manufacturing

Mainly for the steadily increasing price of the bare titanium, the option of replacing few key elements in the tuner with cheaper material has been recently considered. In particular a tuner version made by stainless steel (SS) and INCONEL has been realized too. This would represent a significant cost reduction in view of a possible future use of a steel He tank when the technology will allow solving the problems of welding titanium to stainless steel. A standard AISI 316 alloy is used for the tuner rings while stronger alloy, INCONEL 718, has been chosen for the realization of blades. FEM analysis has been performed also in this case and the results are summarized in Table 10 and compared to previous results.

| geometry | Material | Limit load stressed state | Max load before plastic strains | Limit load non stressed | Buckling load non deformed state | Limit load final | Stiffness | Tuning range cavity disp. |
|---|---|---|---|---|---|---|---|---|
| | | N | N | N | N | N | kN/mm | mm |
| Original | Ti – gr2 | 786 | 709 | 669 | 427 | 223 | 6.49 | 1.1 |
| New | Ti – gr2 | 486 | 456 | 496 | 290 | 162 | 5.43 | 1.5 |
| New | Inconel 718 | 824 | 693 | 804 | 519 | 268 | 10.2 | 1.5 |

Table 10. - FEM results for INCONEL single blade with new design compared to previous results

Analysis confirmed that INCONEL blades have higher stiffness and load limit if compared to the titanium solution. The former parameter moreover, although positive for the tuning operation, leads to a higher torque required to the stepper motor for a given displacement of the central ring. A factor of two resulted from analysis; therefore a force of 800 N has been foreseen as the maximum axial force on the motor. This value is compatible with motors and harmonic drives currently used. To complete the analysis of the stainless steel option for the new Blade Tuner, it must be considered that, until homogeneous He vessels will be available, the different thermal contractions between tuner assembly and Ti or Nb parts must be kept into account. Despite this additional issue, the saving with SS can be

evaluated, as of today, to about 1000 euro absolute for the single tuner prototype and to 5% [18] relative for the large scale production, although this latter cost reduction effect will steeply increase over next years.

From all these considerations and analyses shown, both the titanium and the stainless steel options have been developed and realized for qualification by Zanon, as shown in Fig. 22.

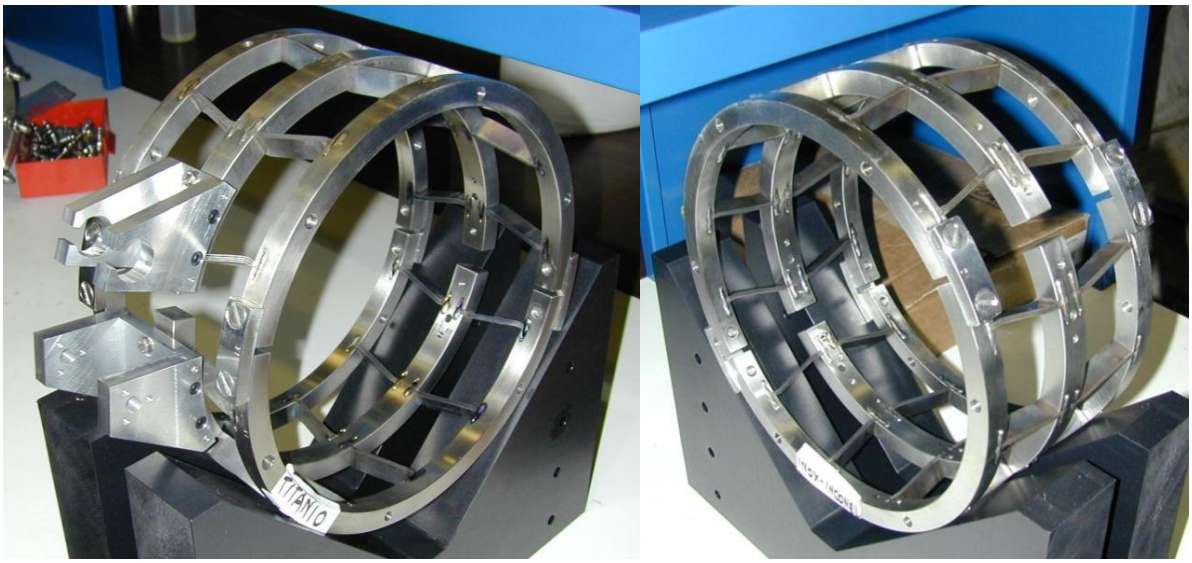


Fig. 22 – Manufactured and assembled Blade Tuners with revised design, titanium model (Slim_Ti, left) and stainless steel model (Slim_SS, right)

## 6.3. New blade tuner mechanical tests at LASA

Before the cold test, preliminary measurements have been performed at LASA laboratory using the dedicated tuning facility that hosts a Nb single cell TESLA cavity. Both INCONEL and Ti (further on referred as Slim_SS and Slim_Ti respectively) model of the new design Blade tuner have been tested, together with the Superstructure tuner device (SuTu_IV) that has been considered as the reference version.

During tests, load button sensors were installed for force measurements while micrometer gauges were used for relative displacement. The complete setup for the first installation of the Slim_Ti tuner is shown in Fig. 23. Gauges were placed only at the piezo side of each tuner since the other flange is fixed to the table by means of a rigid constraint. For each tuner installed, four gauges have been placed on the moving side of the tuner, two of them were always set in the proximity of each piezo support while the remaining two were set around the ring. The number of turns performed by the motor CuBe screw has been measured and assumed as the input variable for the measurements.

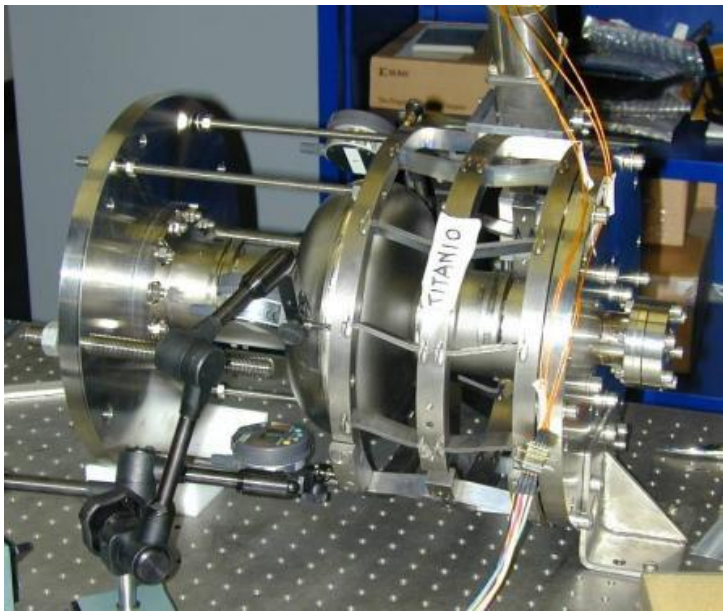


Fig. 23 – Slim_Ti tuner installed in test facility

The first performed test investigated the unloaded cinematic performances of each tuner model. A comparative displacement result is shown in Fig. 24, where the average readout of the "piezo" gauges is considered. Gauge readouts were anyway completely consistent all over the tuner ring.

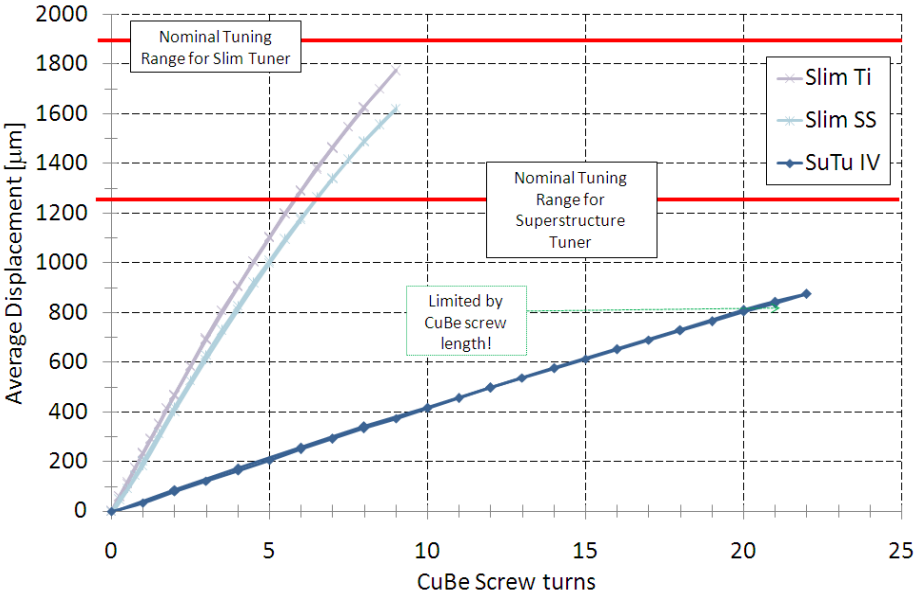


Fig. 24 - Displacements vs. screw turns curve for the unloaded case

All tuners behaved as expected, even if the tuning range for the SuTu_IV tuner was actually limited only by the length of the CuBe screw.

After these first tests, an external constraint has been added in order to reproduce the static load transferred to the tuner through the piezos. With the use of an appropriate combination of spring washers coupled to the force sensor available, the external stiffness (i.e. the stiffness of the tuner constraining mechanism) in its real environment has been faithfully reproduced (~3 kN/mm, dominated by cavity stiffness). When higher loads were needed for the test, the combination of spring elements has been changed to increase the overall value. The exact

external stiffness for each data series has been anyway measured and it is shown. Loaded and unloaded displacement results are reported in Fig. 25 and Fig. 26.

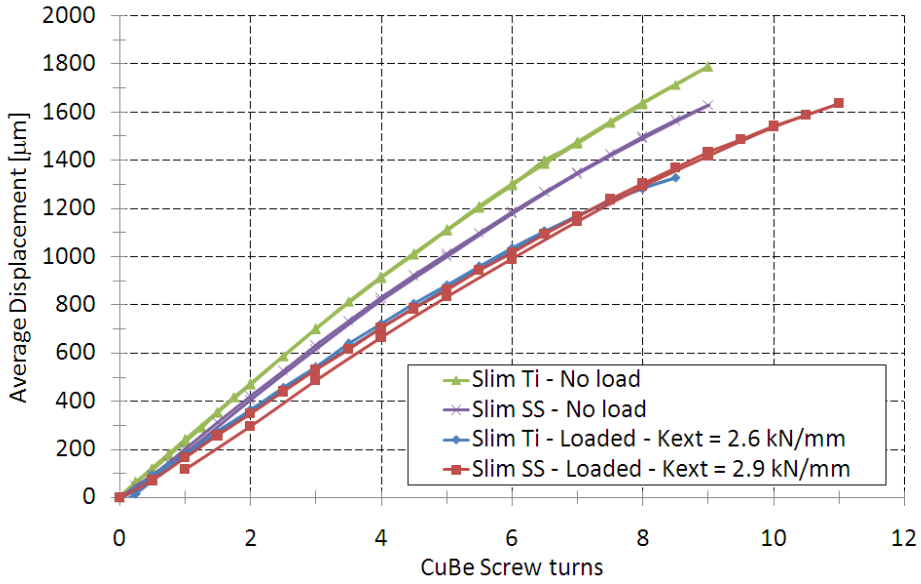


Fig. 25 – Loaded vs. unloaded curves for new design Blade Tuners

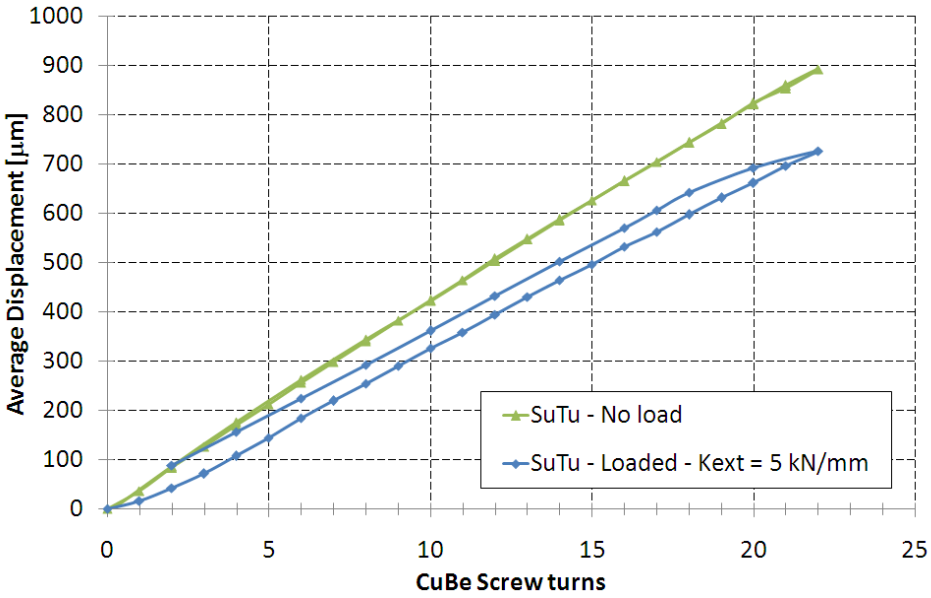


Fig. 26 - Loaded vs. unloaded curves for SuTu_IV tuner

The new tuner devices showed similar loaded responses, and the loaded test successfully confirmed the expected hysteresis lowering in comparison to the SuTu_IV model, in which non-elastic deformations are more likely to occur due to the leverage kinematics itself.

Buckling of few blades appeared for both new design tuner models at high load level. Slim_SS tuner anyway proved to be able to sustain higher load level, repetitively performing a load limit of 6.15 kN, consistent with the tuner requirements. Maximum load capability is actually limited almost completely by the blades placed closer to piezo holders that bear the main part of the generated force. As a reference, buckling deformation experienced by these blades in the Slim_SS loaded test is shown in Fig. 27.

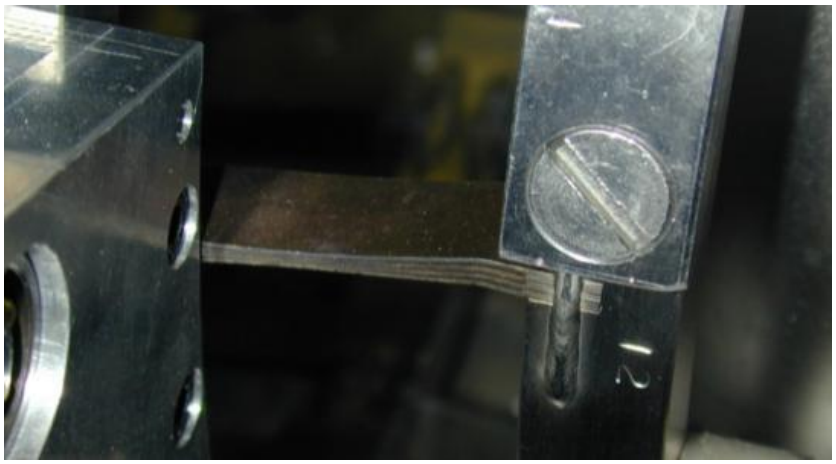

Fig. 27 – Buckling of most sensitive blades for the Slim_SS tuner over load limit

The SuTu tuner instead was loaded and moved up to a total load of 8 kN and no buckling appeared, due to the considerably higher number of blades. In Fig. 28. the generated force is plotted against the total tuner elongation for all tuners.

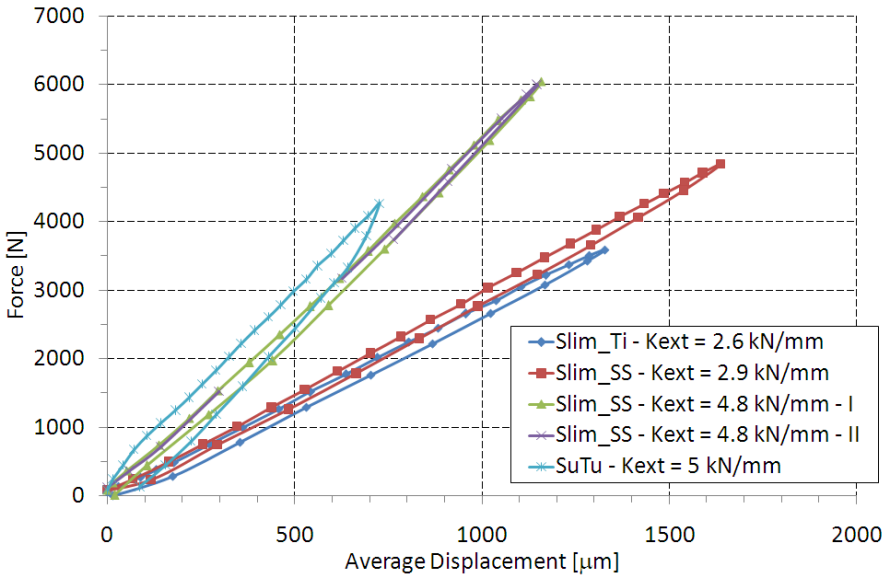


Fig. 28 - Compression force vs. displacement curves

For the SuTu tuner, a second measurement has also been performed with a static preload added via the piezo screw rods, in order to reach higher load values. Results are shown in Fig. 29.

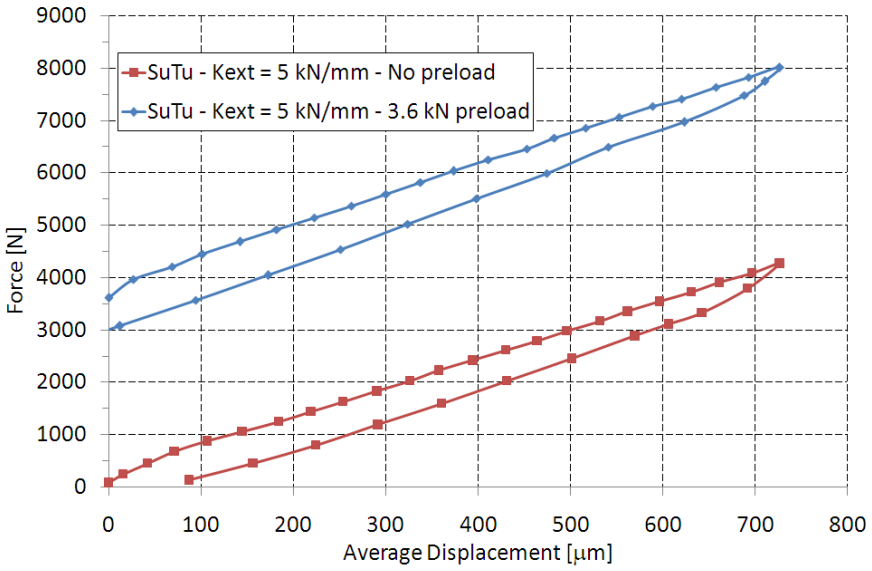


Fig. 29 - Compression force vs. displacement curve for the SuTu_IV tuner

Finally, to complete the analysis of acquired data, for each CuBe screw turn the difference between unloaded and loaded displacement of each tuner has been computed. This is an estimation of the passive compression (shortening) of the tuner itself at a given load value, therefore allowing to estimate the stiffness of each tuner. Results are shown in Fig. 30.

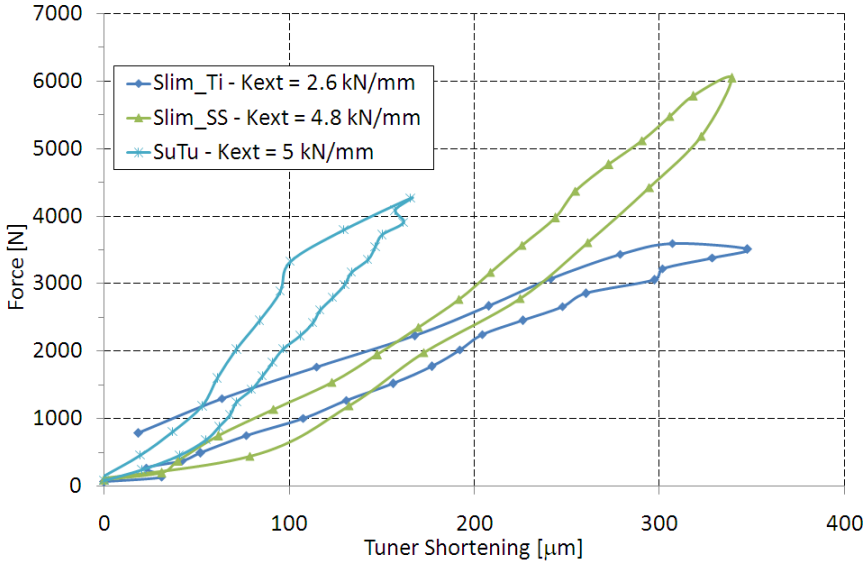


Fig. 30 - Compression force vs. shortening curves

These curves reveal that the stiffness of each tuner has its minimum value for small shortening (max blade angle) and then reaches its typical value over the full range. Therefore, interpolating over 0 - 25 % of max compression for minimum stiffness and over 25 - 75 % for mean stiffness, the results are:

$$Slim\_Ti : K_{mean} = 11\ kN/mm\ ;\ K_{min} = 9.5\ kN/mm$$

$$Slim\_SS : K_{mean} = 22\ kN/mm\ ;\ K_{min} = 12.5\ kN/mm$$

$$SuTu\_IV : K_{mean} = 32\ kN/mm\ ;\ K_{min} = 17.5\ kN/mm$$

These values should be compared to a goal stiffness value of 25 kN/mm that can grant the actual piezo-to-cavity displacement ratio of 74 %, that is also the value that has been measured experimentally for the first SuTu tuner.

Numerical FEM simulations have been also performed in order to verify the obtained results, both for unloaded and loaded tuner constraints, for the Slim_Ti and Slim_SS (unloaded) and Slim_Ti (loaded) tuners. The results are respectively shown in the following pictures (Fig. 31 and Fig. 32 respectively).

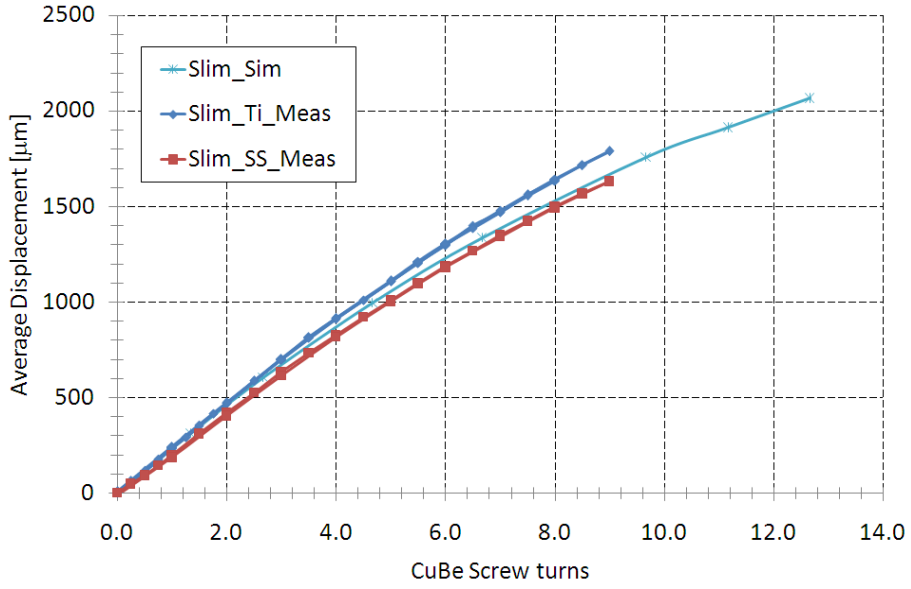


Fig. 31 - Comparison of experimental and numerical data at the piezo position for the unloaded case

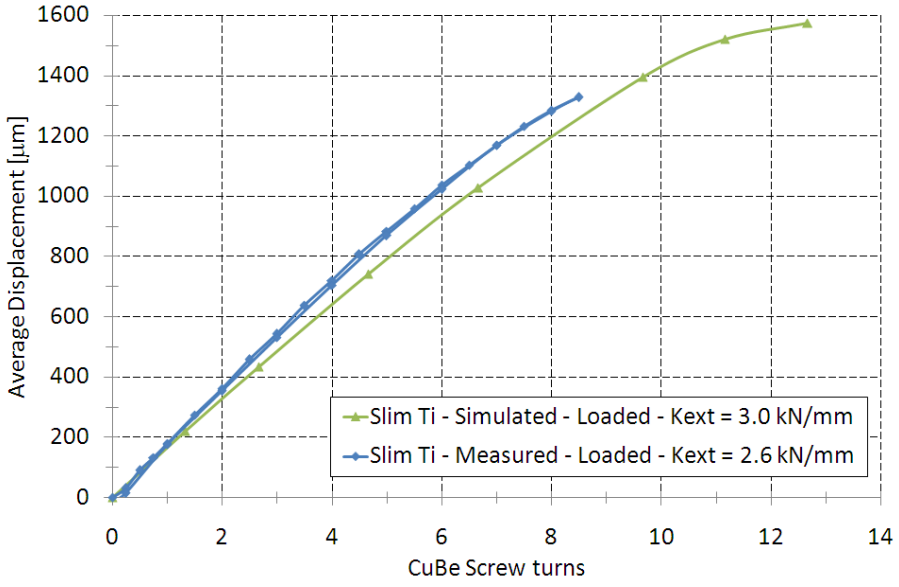


Fig. 32 - comparison of experimental and numerical data at the piezo position for the loaded case

# 7. Final design update and installation procedure

The results of tests performed at room temperature on the available tuner models confirmed that the INCONEL – Stainless steel version of the new design Blade Tuner

behaves as expected, therefore it has been chosen for first cold test to be performed in the horizontal cryostat CHECHIA. Some additional modifications in the design have been anyway implemented, consisting of the realization of few additional pieces.

In order to adapt the Slim_SS tuner to the rings design of the old modified He tank available for cold test in CHECHIA[2], four stainless steel half rings have been realized to be sided to both the existing outer *rings of the t*uner. The Blade Tuner 3D model with these additional elements installed is visible in Fig. 33.

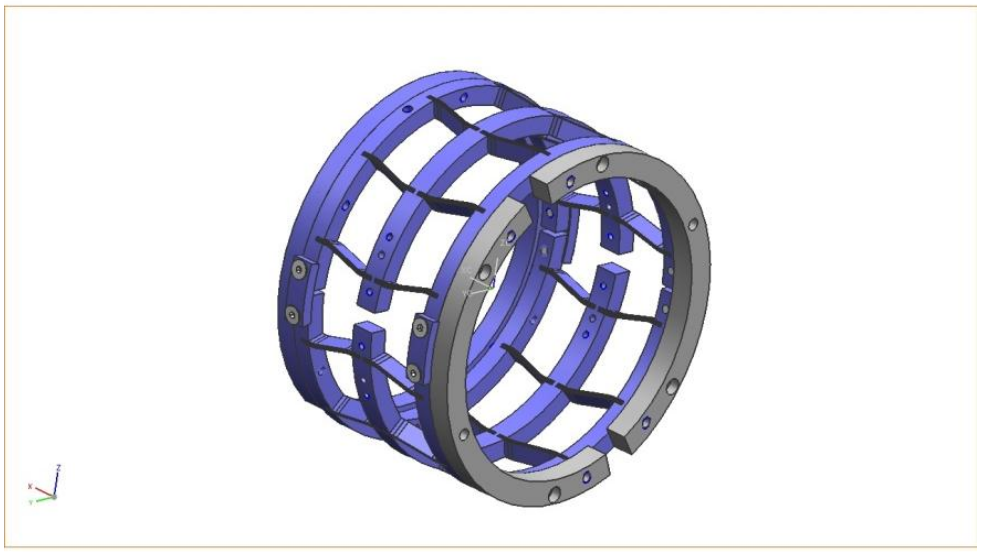

Fig. 33 – The additional adaptation rings, in grey, installed for the new design Blade Tuner

Moreover, FEM analysis of the Slim_SS tuner with the additional outer ring installed gave as result an expected increasing of 10 % in the maximum sustainable load limit. Therefore a threshold value of 6.7 kN will be further on considered as the maximum achievable overall load on the tuner. Finally, see Table 11 for a summary of the results, each foreseen load case during test, starting from the installation up to the operation, has been considered and simulated in order to estimate, for each single case, the compressive and tensile loads in the system together with the corresponding cavity frequency. The starting frequency of this analysis is the measured value after the last cavity tuning operation, before the He tank integration. It is assumed and expected that the installation of the tuner itself on the 9-cell cavity would don't introduce any further loading and frequency variation, except for the piezo preloading. The stepper motor is installed and then kept in the starting point of its tuning range during both installation and cool-down (i.e. no additional motor screw turns before operative conditions are reached).

The analysis is based on results and parameters of the mechanical spring-mass model already developed for the system and discussed previously [12]. In addition the analysis has taken into account the presence of safety bolts properly installed on the support screw rods, as already introduced. Therefore these bolts are engaged when tensile loads are generated on the tuner. Finally, simple FEM simulations were used to estimate the reactive force of the cavity when subjected to a pressure difference of 1 bar, after evacuating the beam pipe. The following table summarizes analyses results for each foreseen load condition. The peak compressive and tensile loads during cooldown procedure are highlighted. A value of 1.15 bar

[2] Tuner and He tank sides had different layouts for the screwed holes needed for tuner installation, the existing layout was initially realized in order to host the SuTu tuner.

has been considered for the peak pressure during the liquid He transfer to the He tank[3]. Compressive load values are negative.

| | Load case | Temp. cavity K | Pressure beam pipe bar | Pressure He tank bar | Pressure isovac bar | Force tuner kN | Force cavity kN | Force Each Piezo kN | Frequency cavity MHz |
|---|---|---|---|---|---|---|---|---|---|
| 1 | start | 300 | 1 | 1 | 1 | 0 | 0 | 0 | 1297.333 |
| 2 | tuner assembly and piezo preload | 300 | 1 | 1 | 1 | -2.2 | 2.2 | -1.1 | 1297.563 |
| 3 | vacuum in the cavity | 300 | 0 | 1 | 1 | **-2.9** | 2.9 | -1.45 | 1297.913 |
| 4 | iso vacuum in the cryostat | 300 | 0 | 1 | 0 | 2.7 | 2.1 | 0 | 1298.07 |
| 5.1 | He injection | 300 | 0 | 1.15 | 0 | 3.3 | 2.2 | 0 | |
| 5.2 | LHe in the tank | 4 | 0 | 1 | 0 | **4.55** | 0.95 | 0 | 1299.94 |
| 6 | superfluid He / min of tuning range | 2 | 0 | 0.02 | 0 | -1.1 | 1.1 | -0.55 | 1299.75 |
| 7 | superfluid He / max of tuning range | 2 | 0 | 0.02 | 0 | -5.5 | 5.5 | -2.75 | 1300.1 |

Table 11 – analyses and simulation of each tuner load case, from assembling to cool-down

Such analyses have confirmed that it is correct to expect not to exceed the maximum load sustainable by the Slim_SS tuner and that, moreover, the goal frequency of 1300.0 MHz should be achievable and close to the middle of the tuning range, as designed.

It is also shown that the peak tensile force must be actually considered as the most critical transient situation, since up to more than 4.5 kN of tensile force is expected to act on the tuner. Given that the cavity is already almost not sensitive to this force, since safety bolts transfer it almost completely to the tuner, the mechanical contact with piezo actuators must be anyway preserved and excessive loosening must be avoided. While a definitive solution for this problem is under development, a provisional but effective remedy during the first tests has been adopted. This is accomplished using two helicoidal springs that have been installed below the piezo holder by the tuner side, as shown in following Fig. 34.

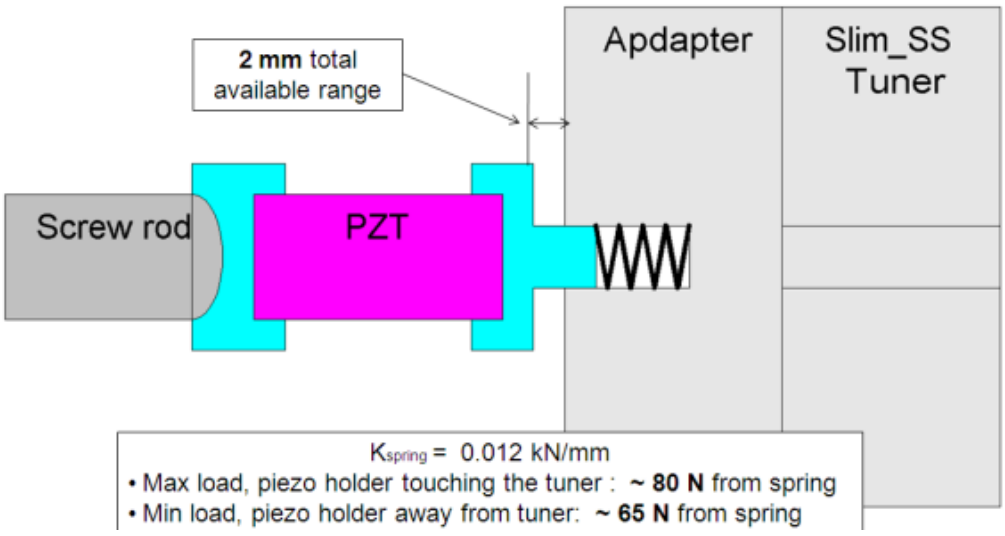


Fig. 34 – Basic design of piezo holder spring insertion for the new tuner design

[3] This value is although very difficult to predict and to control, some more experience and statistics is needed.

Finally, the complete set of new Blade Tuner (Slim_SS) assembly elements, corresponding to the tuner in its final version for DESY cold test inside CHECHIA, is shown in Fig. 35.

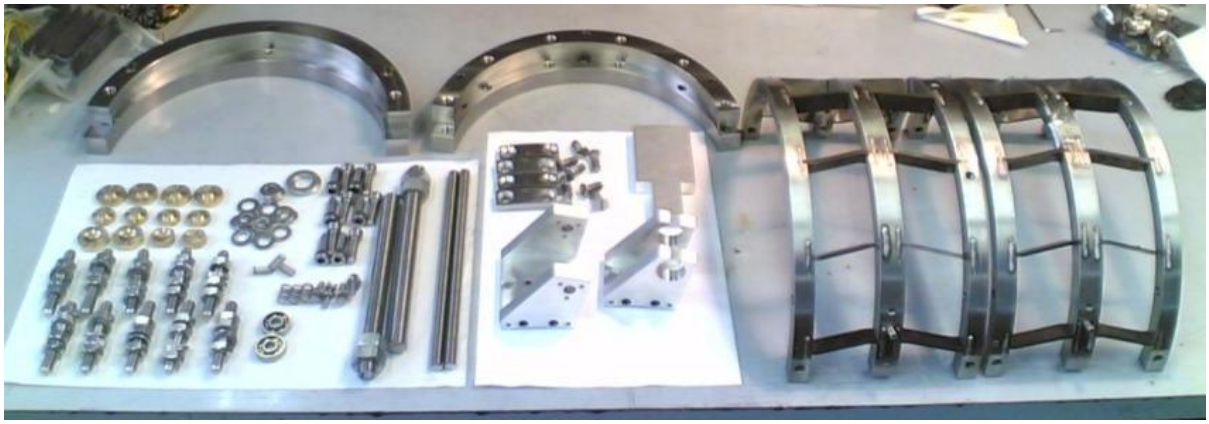

Fig. 35 – The tuner parts ready to be assembled before the DESY cold test

## 7.1. New blade tuner cold test at DESY

In order to test the coaxial tuner in CHECHIA [13], the Zanon n°86 cavity, or Z86, has been used. From April to June 2007, the Z86 cavity has been prepared for cold test [24]. End dish welding has been done at the Lufthansa facility[4] while the modified He tank, with the insertion of a central bellow, has been then installed in DESY. The cavity has moreover sustained the usual DESY acceptance test procedure, including mechanical qualification test and RF test in vertical cryostat. Summary of main Z86 cavity properties and performances, as emerging from those former tests are reported in Table 12.

| **Cavity** | **Z86** | |
|---|---|---|
| Manufacturer | Zanon, I | |
| Arrival at DESY | 22/04/05 | |
| Weight | 26.55 | kg |
| BCP sessions | 1 | |
| Material removed by BCP | < 10 | μm |
| EP sessions | 3 | |
| Material removed by EP | 242.1 | μm |
| Baking | 800° , 2h | |
| | 127° , 48h | |
| RRR | 296 | |
| $E_{acc}$ , V1 | 24.5 | MV/m |
| $Q_0$ , V1 | 1.8 E10 | |
| Field Flatness , last tuning | 97 | % |
| Frequency , last tuning | 1297.333 | MHz |

Table 12 – Summary of Z86 cavity treatments and performances

Finally the Z86 cavity was ready for blade tuner installation, and cold tests inside CHECHIA have been scheduled and performed in weeks # 35 and # 36, September 2007.

[4] Lufthansa Gmbh, Hamburg. A special EB welding machine is used for end dish integration due the high number of degree of freedom (DoF) needed.

### *7.1.1 Cooldown and warmup results*

Starting from September 4th 2007, the installation of the Slim_SS Blade tuner on the full Z86 cavity has been carried through so that in two days the whole setup has been installed in CHECHIA and the test session started.

In order to remove security bars between the He tank rings and install the tuner, beam pipe vacuum has been removed and cavity has been filled with Ar gas at 1 bar pressure. Vacuum in the beam pipe has then been restored right before the insertion in CHECHIA[5]. The first frequency check right before tuner assembling revealed an higher value, by an amount of around 100 kHz, compared to the last available measure. This frequency difference, between the value reported in Table 12 and the value measured just before the test, is mainly due to the fact that during bead-pull operation on the tuning machine, when last frequency value has been measured, both bead and its wire were enclosed in plastic tube, introducing a frequency shift of -80 kHz. Additional -20 kHz can be accounted to the Argon gas different dielectric constant with respect to the Air. The He tank welding procedure instead produces a negligible frequency shift, lower than 10 kHz. Anyway, since the initial cavity frequency was higher than expected, a lower preload has been set on piezo actuators, two NOLIAC 40 mm, in order to reach the correct frequency value for load case # 2, Table 11. This because one of the test goal is to tune the cavity to the nominal 1300 MHz resonant frequency value at 2K.

A stepper motor from Sanyo inc. has been installed provided with harmonic drive gear box. Safety bolts on the four support screw rods have been installed, two on each side of the He tank ring. As foreseen from tuner design the distance between these safety bolts and the outer side of the ring has been set as accurately as possible toward the goal value of 0.6 mm. Unfortunately, this calibrated installation suffered from significant error and the actual distance value could be as high as 1 mm[6]. Finally, a μ-metal foil has been adapted to fit the installed tuner and provide magnetic shielding to the cavity.

The main steps of the tuner assembling and installation in CHECHIA are shown in the following pictures.

Fig. 36 – Z86 and modified He tank with support disks and bellow, ready for Blade tuner installation

[5] Both operation on beam pipe volume, Ar refilling and vacuum pumping, has been performed in the Halle III clean room.

[6] This issue, actually related to the difficulties experienced during bolts installations by hand, will be overcame using proper devoted tools and solutions under designing.

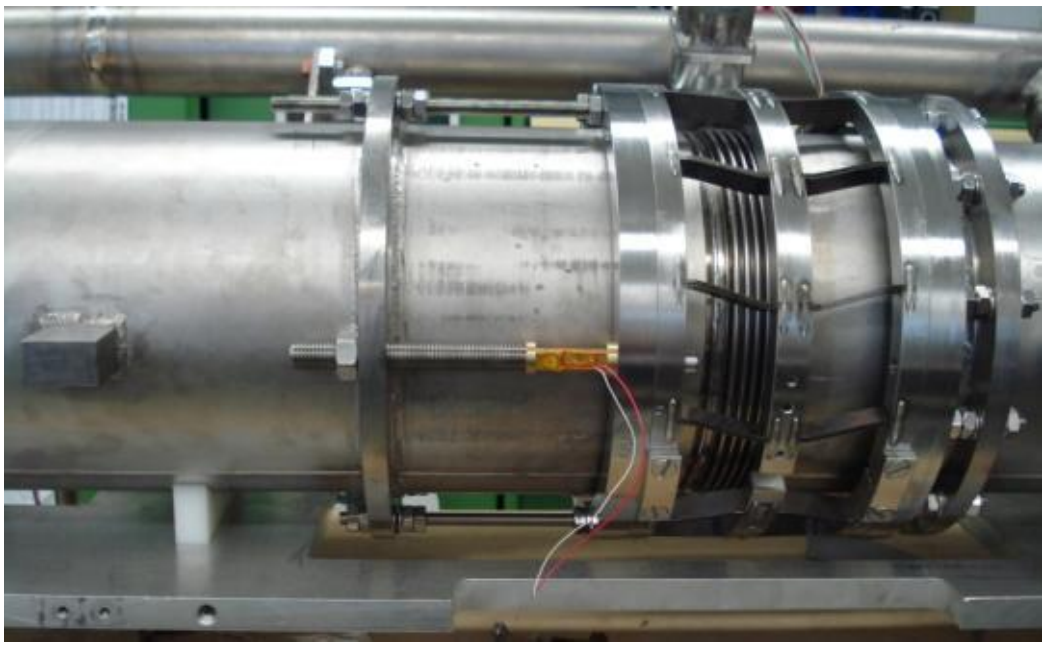

Fig. 37 – The Slim_SS Blade tuner completely installed; piezo actuators are in place and preloaded.

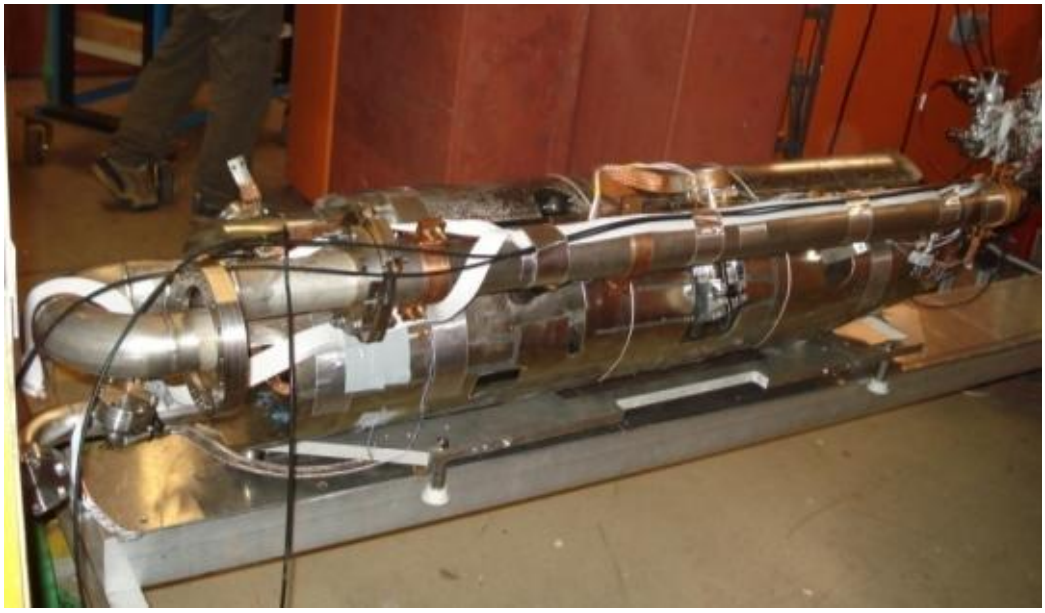

Fig. 38 – Z86 right before insertion in CHECHIA, the magnetic shielding is visible around the He tank

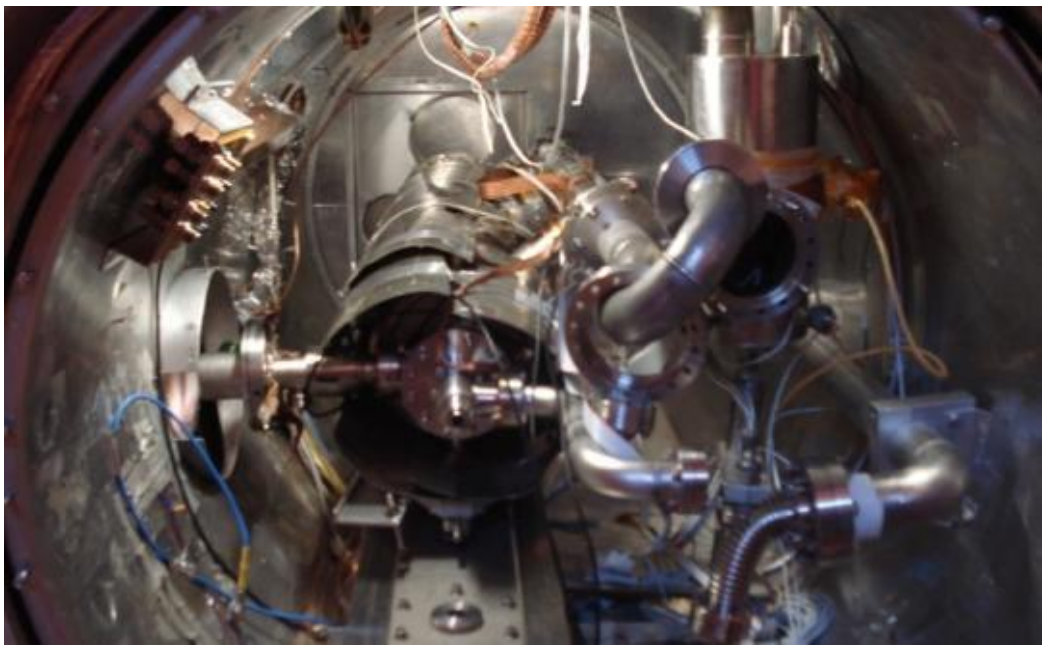

Fig. 39 – Z86 installation in CHECHIA completed, before start of cold test

During the entire assembling procedure until the insertion in CHECHIA, both cavity frequency and piezo actuators static capacitance values have been measured (from here on piezoceramic actuators will be referred as "piezo 1", on motor side, and "piezo 2", on the other side). Cavity frequency shift, and therefore its length deformation, has been also monitored to determine the final piezo preload through known cavity stiffness. Finally, after the conclusion of main ancillaries installations (diagnostic cables, coupler, vacuum and liquid He refilling) the DESY usual schedule for CHECHIA cold test preparation has been followed:

- Isolation vacuum pumping.
- Coupler warm processing: full power pulse, from 20 μs to 1300 μs.
- Start cool-down: liquid He transfer up to 4 K. More than 2.2 bar peak pressure, for about 5 minutes, has been reached during transfer.
- Pumping over liquid He bath: toward superfluid He, 2 K at 30 mbar pressure. He historic plot is shown in Fig. 40.

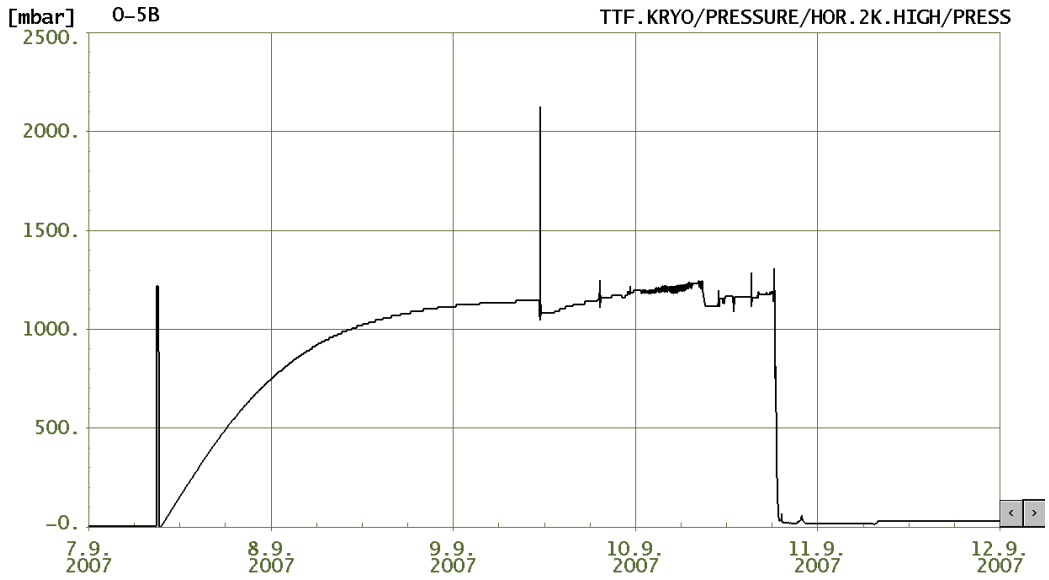


Fig. 40 – He tank pressure sensor historic plot, He filling, pumping over He bath and 2.2 bar peak value are visible

– The cavity is successfully tuned to 1300.0 MHz resonant frequency with the stepper motor: +1.25 screw turns, see Fig. 41 for the spectral line.

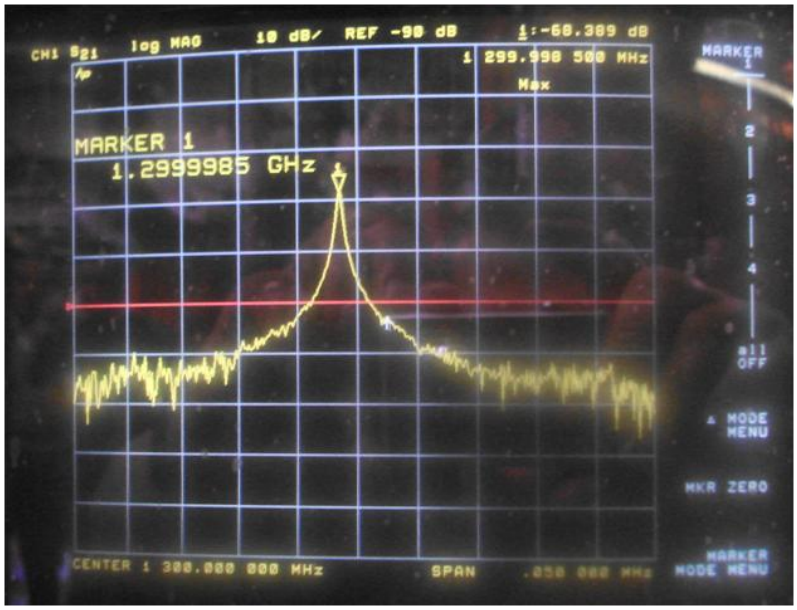


Fig. 41 – Network Analyzer screenshot of the tuned cavity frequency measure

– On resonance coupler conditioning, see Fig. 42 for the historic plot of this procedure.

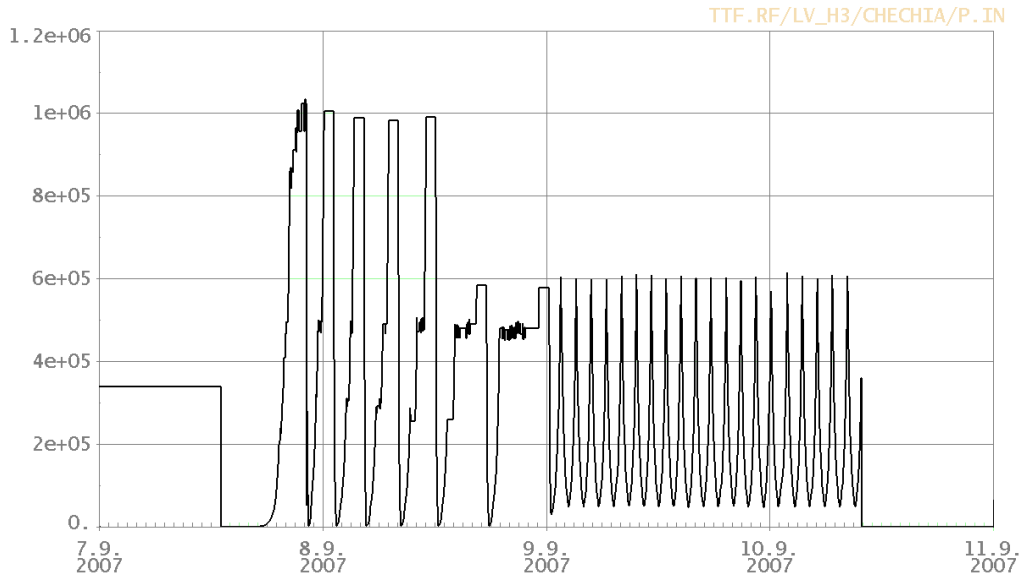


Fig. 42 – Forward power readout historic plot, warm processing up to 9.9.07 then on-resonance cold processing from 9.9.07 on.

The main results concerning recorded parameters from installation to operative conditions have finally been summarized in the following table.

| **Status** | **Cavity frequency** MHz | **Pressure Beam pipe** mbar | **Pressure He tank** mbar | **Pressure isovac** mbar | **Temp. cavity** K | **Piezo Static capacity** 1 - μF | 2 - μF |
|---|---|---|---|---|---|---|---|
| Start | 1297.427 | 1000 - Ar | 1000 | 1000 | 300 | | |
| Tuner on | 1297.445 | 1000 – Ar | 1000 | 1000 | 300 | 9.11 | 8.81 |
| Piezo preloaded | 1297.567 | 1000 - Ar | 1000 | 1000 | 300 | 9.39 | 9.04 |
| Ready to CD | 1297.842 | 0 | *1000* | 1000 | 300 | 10.23 | 10.04 |
| CD done, stable 4K | 1300.191 | 0 | 1200 | 0 | 4 | 3.87 | 3.34 |
| Pumping 1 | 1300.135 | 0 | 500 | 0 | 3 | | |
| Pumping 2 | 1300.045 | 0 | 200 | 0 | 3 | | |
| First 2 K | 1299.996 | 0 | 30 | 0 | 2 | 3.65 | 3.1 |
| Stable 2 K, + 1 d | 1299.974 | 0 | 30 | 0 | 2 | 2.97 | 2.65 |
| Long run 2 K, + 4 d | 1299.978 | 0 | 30 | 0 | 2 | 2.25 | 2.3 |

Table 13 – Summary of all measured parameters during Z86 preparation and cooldown

As previously reported, a preload force lower than the optimal design value, has been set on piezo actuators due the different cavity starting frequency. The preload can actually be estimated observing, from Table 13, that around 120 kHz frequency displacement has been forced on the cavity via the screwed piezo support rods, corresponding to less than 0.6 kN preload for each actuator (approx. one half of the goal value).

Also the final cavity frequency, when stable operation conditions were reached, resulted to be higher than expected from previously presented computations, that were mainly based on the amount of information collected at DESY over different CHECHIA cooldown operations, but with a different tuner. The final frequency revealed to be higher by an amount of 230 kHz, three main contributions to this frequency shift can be extrapolated from data:

1) *70 kHz less than expected* for the frequency increasing due only to vacuum in the cavity, +280 kHz instead of +350 kHz.

2) *320 kHz more than expected* for the frequency increasing due to 300 K to 4 K cooldown, +2.35 MHz instead of +2.03 MHz.

3) *20 kHz more than expected* for the frequency lowering due to 4 K/1bar to 2 K/20 mbar cooldown, -210 kHz instead of -190 kHz.

Nevertheless, although higher than expected (-70 +320 -20 = +230 KHz difference), the cavity frequency remained below the 1300.0 MHz threshold at the lower limit of the tuning range, therefore the nominal operating frequency has been successfully reached.

Finally, on September 11$^{th}$ 2007, the Z86 cavity was ready for tuner and piezo cold test, performing more than 23 MV/m accelerating gradient, in pulsed operation with 1.3 ms RF pulse length.

### *7.1.2 STATIC TUNING RANGE TEST*

After stable 2K He bath conditions were reached, the measurement of the Slim_SS tuning range has been performed, using a vector Network Analyzer to measure the cavity resonant frequency while moving the tuner stepper motor.

All collected points concerning the tuning range are shown in the following plot of Fig. 43. The tuner sensitivity, namely the frequency shift vs. screw turn, has also been computed from data and reported in next Fig. 44.

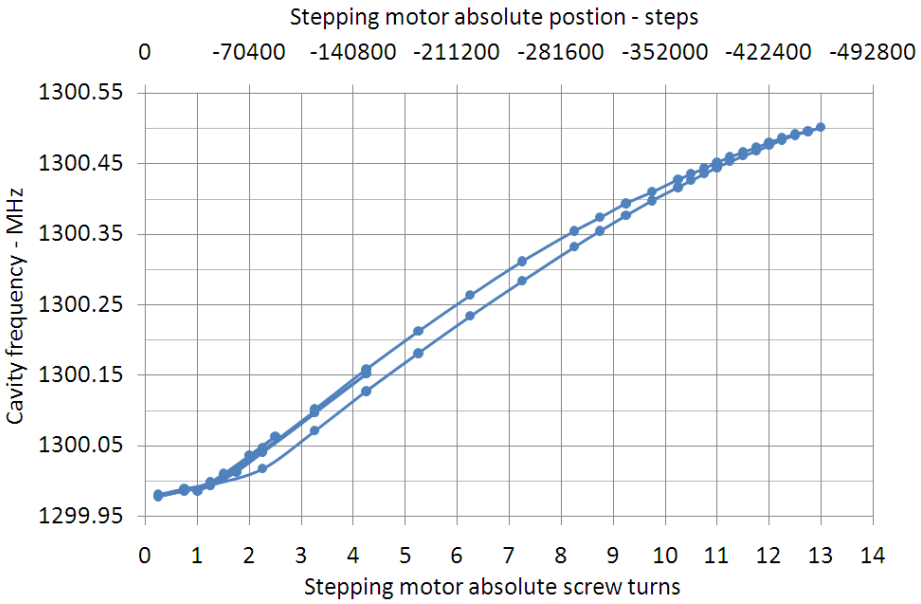


Fig. 43 – Slim_SS Blade tuner tuning range, 13 complete screw turns.

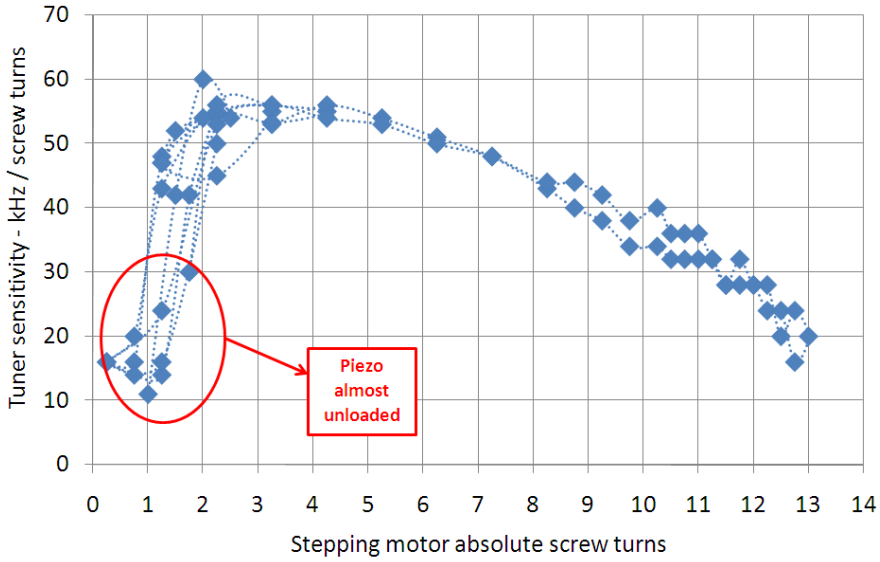


Fig. 44 – Frequency shift vs. screw turns sensitivity for the Slim_SS Blade tuner

The experimental data collected confirmed that the Slim_SS Blade tuner performed the expected tuning range of 520 kHz, over 13 complete motor screw turns and confirmed also the peak sensitivity value of 50 kHz per screw turn expected by tuner design.

The loading force generated by the cavity, that reached a peak value of 5 kN at the higher end of the tuning range, has been successfully borne by the tuner. The smooth and repetitive behavior of cavity frequency around the highest load value confirmed that no buckling occurred to tuner blades.

A visible hysteresis is anyway present in the plot of Fig. 43, where a peak frequency difference of 30 kHz is present after a complete load cycle, around screw turn # 2. This value actually matches the hysteresis shown by the same Slim_SS tuner for the first loaded cycle at room temperature at LASA Laboratory, shown in Fig. 28, where about 0.1 mm of tuner displacement difference can be deduced corresponding to approximately 30 kHz for the cavity. Moreover it must be underlined that the tuner performances in term of hysteresis reduction has been considerably improved with the new design if compared to the previous design, mainly thanks to the removal of the stepper motor leverage. Shown hysteresis can be anyway justified by the need of a “load conditioning” of the tuner itself, since the installed setup reached these high load values for the first time during this test, as will be shown in the following tests at BESSY.

The effect of the undesired frequency offset is even more evident from the data plots presented. Two complete turns were needed from the lower end of tuning range for piezo actuators to be in complete contact with the tuner in order to reach the nominal tuner sensitivity. In this range, springs below piezo holder were keeping actuators firmly in place and only slightly detuning the cavity (generated force below 100 N).

### *7.1.3 LORENTZ FORCE DETUNING COMPENSATION PERFORMANCES*

Before the LFD compensation test started, the cavity has been tuned to the nominal 1.3 GHz resonance frequency using the stepper motor. As told before, this frequency is reached just a little bit further the lower frequency position of the tuning range. Mechanical preload available for piezo in this case is, as said, lower than the optimal value for LFD

operations [8], [14]. Actuators were anyway still effective; and during the test the preload force has been increased to investigate its effect on the effectiveness of the compensation.

In order to determine the correct pulse timing for Lorentz force detuning compensation, a sweep around different pulse timing values has been performed while acquiring resulting cavity detuning. The same pulse used in CMTB module 6 piezo test, single sinusoidal pulse 2.5 ms width, has been set up, also to ease comparison of results.

The results of this piezo timing effect test are graphically summarized in Fig. 45.

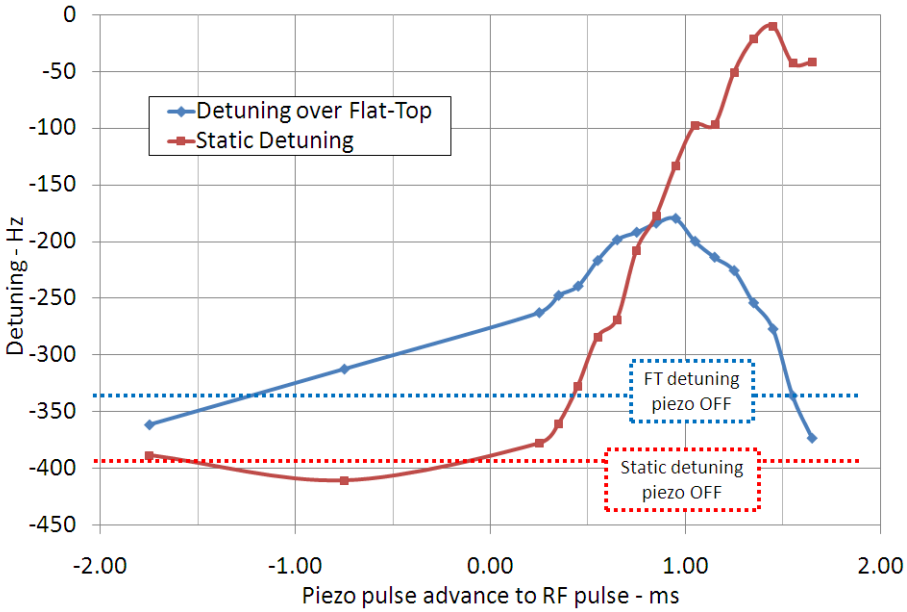


Fig. 45 – Analysis of the piezo pulse advance effect on cavity detuning, Slim SS tuner cold test

Both static detuning and flat-top detuning curves behave as expected, revealing that the best timing setting for the "1st oscillation compensation scheme" requires in this case a piezo pulse advance of *0.85 - 0.95 ms* with respect to the RF pulse. These values are actually comparable to the ones from module #6 TTF piezo tuner analysis [12], with 0.65 ms advance. For subsequent LFD compensation measurements, an advance value of 0.95 ms has been set.

Assuming that cavity stiffness value, 3 kN/mm, is preserved passing from room temperature to the actual cold environment, the overall preload available for both piezo actuators in the initial test setting, 1.25 screw turns, was lower than 0.2 N. Therefore an additional LFD compensation test has been performed at higher cavity frequency, when available total load was 1.2 kN, corresponding to 2 additional screw turns and a frequency shift of about 100 kHz.

It must be underlined that the expected working point for cavity and piezo actuators at 1300.0 MHz was rather the latter one, as foreseen by load cases simulation already shown. Since, as told before, the initial cavity frequency was 100 kHz higher than expected the piezo preload at the nominal frequency is considerably lower than the designed best working point. Therefore, to reach this point a further frequency shift must be forced so to allow a higher load on piezo actuators.

The entire Lorentz force detuning shown by Z86 cavity at full gradient, in different load conditions, driving piezo 1 alone, driving piezo 2 alone and even driving both piezo in parallel, has been successfully compensated. Plots of cavity detuning and phase of RF probe data are reported in Fig. 46 and Fig. 47. They correspond to the best results obtained in the higher piezo load configuration, (i.e. second load case, 1.2 kN total force). Numerical results from all other measurements have then been summarized in Table 14.

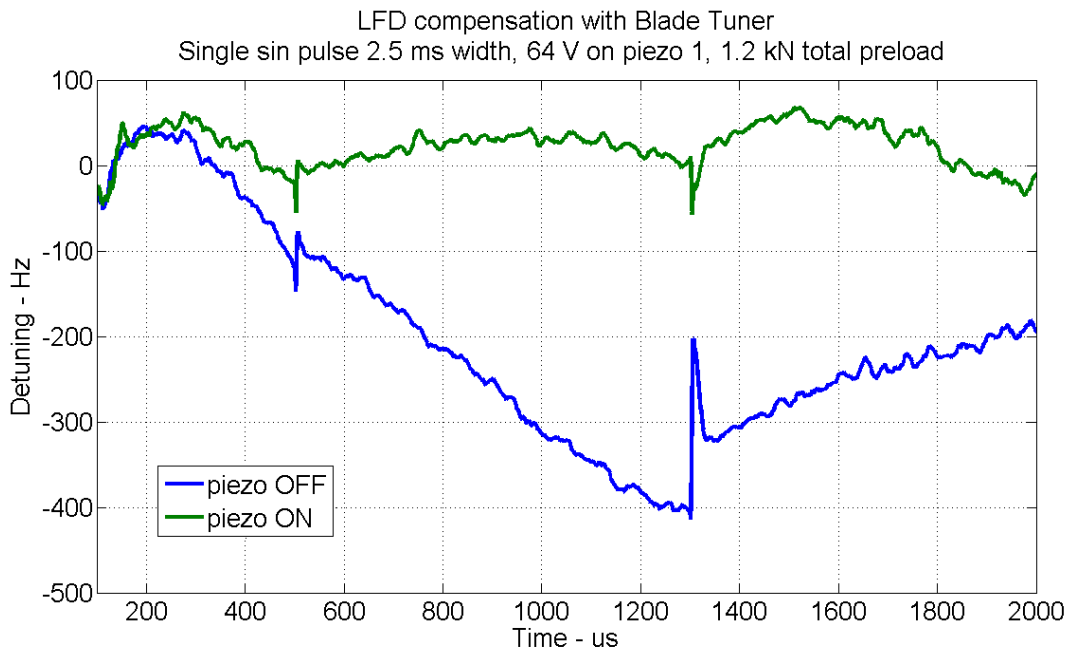


Fig. 46 – Z86 cavity detuning with and without piezo active compensation

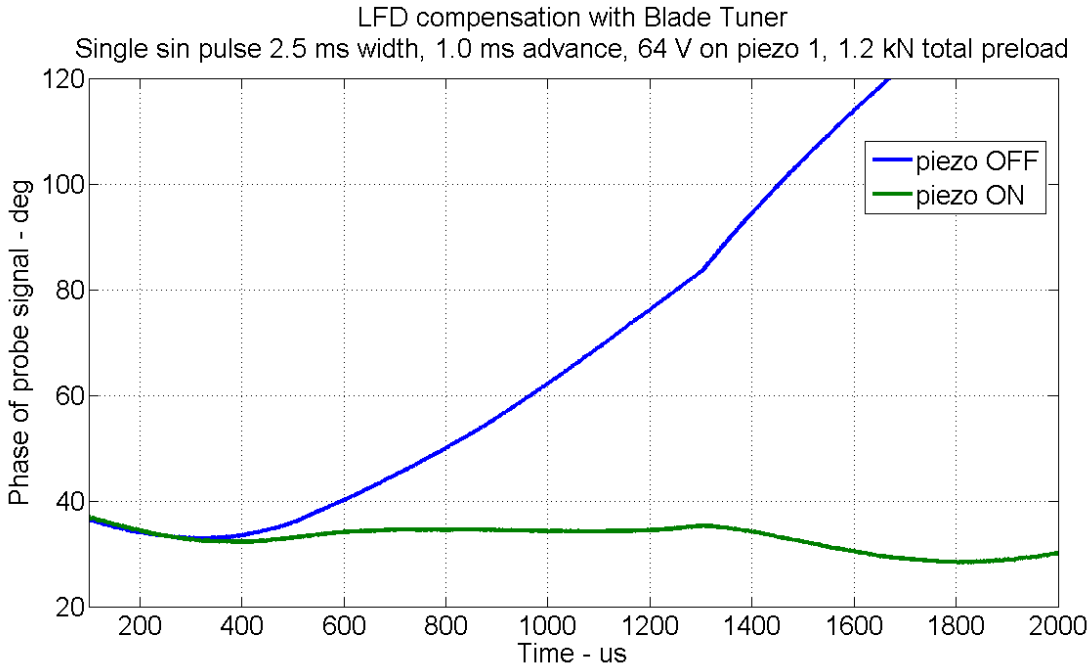


Fig. 47 – phase of Z86 cavity RF probe signal, with and without piezo active compensation

| Used PZT | Gradient [MV/m] piezo OFF/ON | Cavity freq. [MHz] | Total Piezo load [kN] | FlatTop Detuning [Hz] | | Static detuning [Hz] | | Piezo amp. [V] $V_{max}$=200V | Piezo advance [ms] | Comp. FlatTop detuning [Hz] | FlatTop phase stability | FlatTop amp stability |
|---|---|---|---|---|---|---|---|---|---|---|---|---|
| | | | | piezo OFF | Piezo ON | piezo OFF | Piezo ON | | | | | |
| 1 | 23/23 | 1299.988 | 0.2 | -332 | -49 | -392 | -7 | 75 | 0.95 | 283 | +78% | +68% |
| 1 | 23/23 | 1300.097 | 1.2 | -308 | -46 | -326 | 5 | 64 | 0.95 | 262 | +95% | +64% |
| 2 | 23/23 | 1300.097 | 1.2 | -308 | -60 | -326 | 33 | 56 | 0.95 | 248 | +95% | +45% |
| 1+2 | 23/23 | 1300.097 | 1.2 | -308 | -78 | -326 | -83 | 50 | 0.95 | 230 | +66% | +87% |

Table 14 – all results from LFD compensation measurements on Z86 cavity in CHECHIA

Both Lorentz force detuning compensation and a net improvement of RF amplitude and phase stability over the flat-top time window (or "FT", from 500 to 1300 μs) are evident from the reported plots and were obtained with a piezo pulse amplitude well below its nominal (room temperature!) maximum driving voltage value of 200 V, especially when actuators are operated in parallel. Collected data at 1.2 kN load level also revealed that detuning compensation performances are slightly different between piezo 1 and 2, the latter one being more efficient. This behavior was anyway expected. The main contributions come both from the small difference in tuner stiffness, that is asymmetrical by design, and from the piezo preloading procedure itself, right after tuner installation.

LFD values for Z86 cavity without piezo active compensation, as reported in Table 15, resulted to be slightly over the expectations in comparison to usual TTF operation experiences at the same accelerating gradient, although more measurements on different cavities are needed to confirm this issue. It is anyway clear that both the cavity intrinsic LFD reduction and the lower pulse amplitude needed, confirmed that the whole tuner fast tuning system took clear advantage from the increasing of the mechanical preload when cavity is operated closer to the middle of the tuning range.

| Test | tuner | PZT used | load | Δω over FT | $E_{acc}$ | $V_{piezo}$ for Δω compensation | $V/V_{max}$ |
|---|---|---|---|---|---|---|---|
| | | | [kN] | [Hz] | [MV/m] | [V] | |
| ACC6 avg. | TTF | 1 | | 250 | 23 | 45 | 0.375 |
| ACC6 avg. | TTF | 1 | | 300 | 25 | 54 | 0.45 |
| Z86 | Blade | 1 | 0.2 | 332 | 23 | 75 | 0.375 |
| Z86 | Blade | 1 | 1.2 | 308 | 23 | 64 | 0.32 |
| Z86 | Blade | 2 | 1.2 | 308 | 23 | 56 | 0.28 |
| Z86 | Blade | 1+2 | 1.2 | 308 | 23 | 50 | 0.25 |

Table 15 – Comparison of LFD compensation performances between TTF and coaxial tuner test

In order to have a preliminary evaluation of Slim SS Blade tuner performances, the shown data can be compared to the data set from FLASH module #6 tests [12], [19]. Averaging over the cavity performances of the whole module, the latter tests with TTF piezo tuner, revealed a LFD sensitivity of $-0.47 \pm 0.05$ Hz/(MV/m)$^2$, compared to the blade tuner test results of -0.63 and -0.58 Hz/(MV/m)$^2$ with 0.2 kN and 1.2 kN preload respectively. Considering the results of the analytical modeling presented before and the limitations for the test due to the old He tank design, a similar behavior could be expected. It is anyway important that, when the load reaches acceptable values as in the latter case, the $K_L$' for the coaxial tuner installation is still in the order of most sensitive cavities with TTF tuner installed. For further comparative analyses selected results have been summarized in Table 15, where ACC6 average LFD

compensation results have been scaled for an $E_{acc}$ value of 23 and 25 MV/m to correlate them to the coaxial blade tuner test data. For each case both the amplitude of piezo voltage used for compensation and its ratio with the corresponding maximum nominal voltage (120 V for PI_36 piezo in ACC6, 200 V for NOLIAC_40) are shown.

Although more tests and statistics are needed about coaxial blade tuner installation and operation at cold, test results are very good, mainly since the higher LFD sensitivity shown is balanced by a higher piezo fast tuning efficiency in term of driving voltage margins. Moreover a clear improvement on both aspects seems to be confirmed, as expected from design, when increasing the mechanical load on the tuner assembly.

### *7.1.4 "Piezo to piezo" transfer functions*

Both the cavity sensitivity to Lorentz Force and the efficiency of piezo detuning compensation revealed some dependence from the mechanical compressive load generated by the cavity and set by the working point in the tuning range. As a reference, the total generated load over the whole tuning range is reported in next Fig. 48. The force has been computed taking into account, also for the cold environment, the usual room temperature cavity stiffness value of 3 kN/mm.

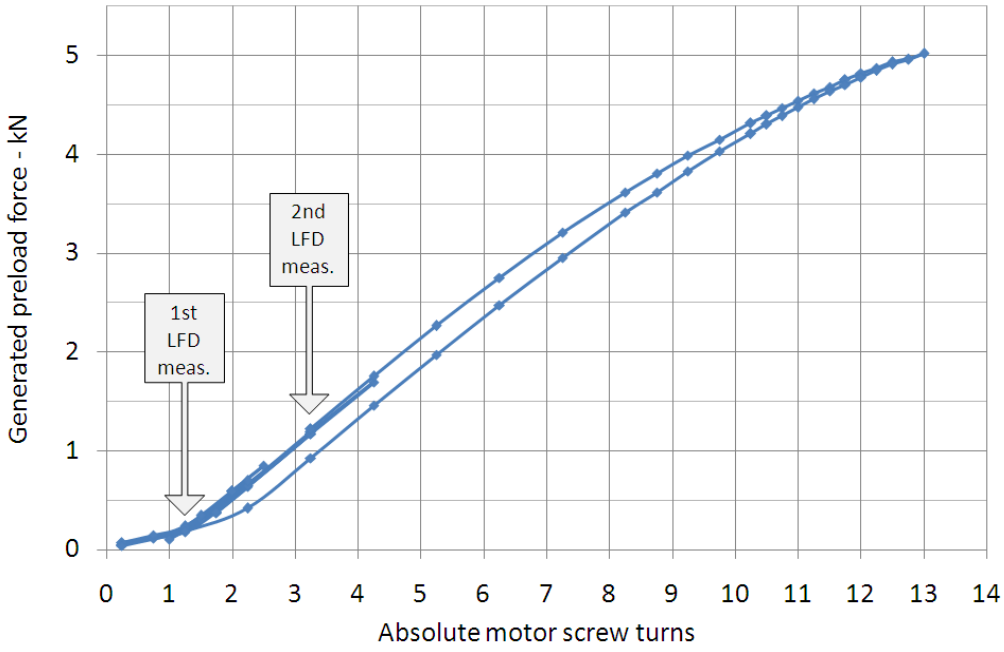


Fig. 48 – Mechanical load generated over the tuning range on the Slim SS Blade tuner

Moreover, a deeper analysis of the mechanical coupling between piezo actuators and their environment has been performed through the measure of the piezo-to-piezo transfer function. The transfer function has been acquired, using the CHECHIA facility lock-in amplifier[7], in different points of the tuning range, therefore at different preload levels. The one corresponding to the highest load is plotted for reference in the next picture, Fig. 49.

[7] The instrument used for this measurement was a SRS840 Lock-In Amplifier from Stanford Research.

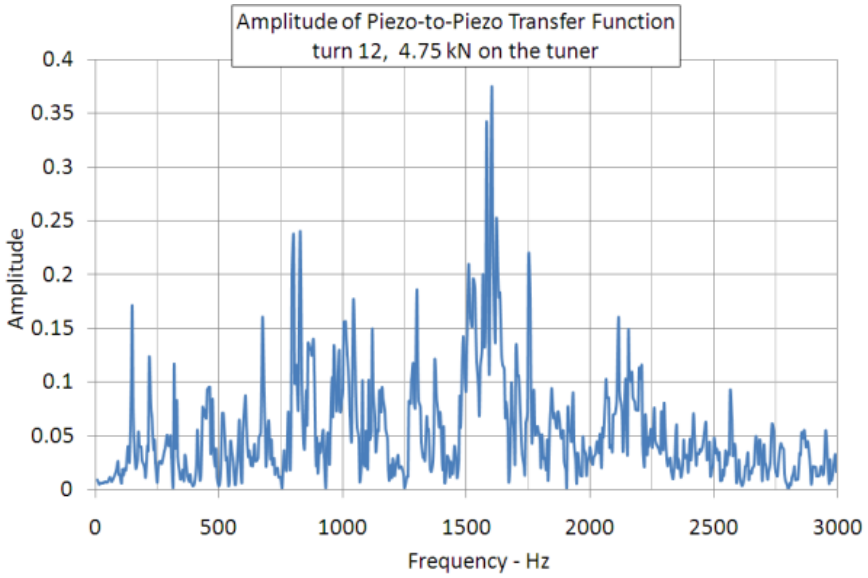


Fig. 49 – Piezo-to-piezo transfer function amplitude

The transfer functions are also influenced by the piezo pre-load (i.e. the mechanical coupling between piezo and cavity). The normalized integral value of the module of the transfer function has been computed over the whole frequency range. The resulting value is then plotted, in the following Fig. 50, as a function of cavity frequency, which is actually proportional to the applied load.

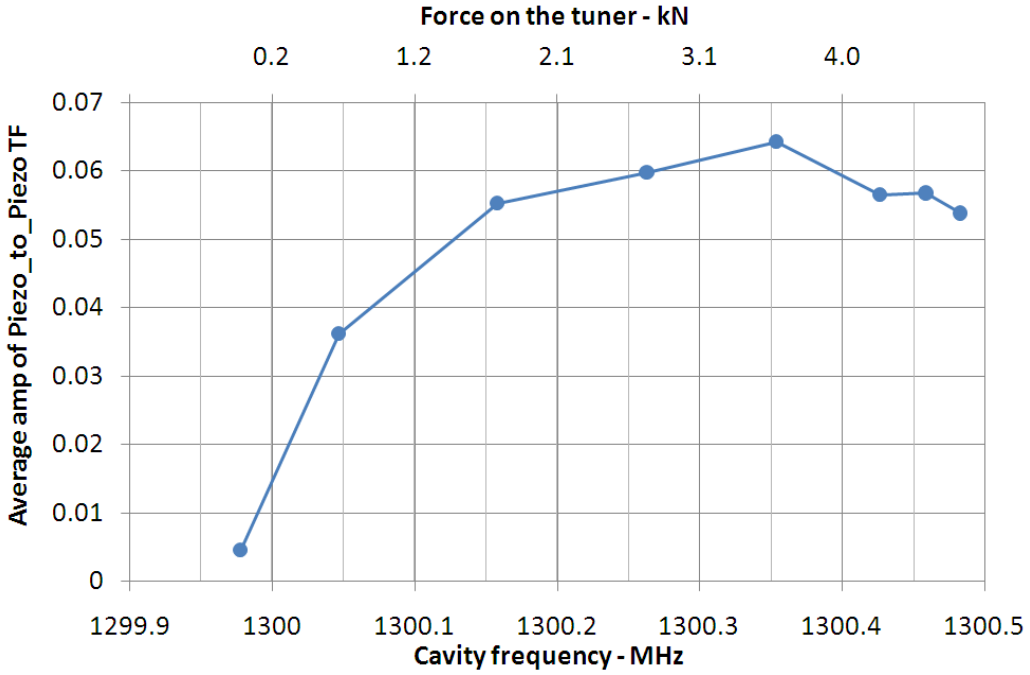


Fig. 50 – Average amplitude of piezo to piezo TF as a function of cavity frequency

The parameter proposed for the analysis seemed to be correctly related to the efficiency of the mechanical coupling between piezo actuators and the cavity. In fact the plot shows that the coupling between the two different actuators gradually increases in the first part of the tuning range, where piezo tests were initially actuated, before reaching, as expected, an asymptotic value when the total load generated by the cavity is higher than about 1.5 kN.

## 7.2. New blade tuner cold test at BESSY

After the test in pulsed regime at DESY, the CW facility HoBiCaT at BESSY [20] allows better investigations on tuning range and transfer functions. A Phytron stepper motor with planetary gear box has been used in place of the former Sanyo stepper motor with harmonic drive gear. The He bath pressure has been stabilized to 16 mbar corresponding to 1.8 K. Additional temperature sensors have been glued on the piezo support (screw side, opposite to the motor), on the Blade Tuner ring (outer ring, close to piezo position, opposite to the motor) and on the stepper motor. Table 16 collect typical values for the temperature sensor of interest as observed during tuner tests, giving the real working point of the main tuner parts. This is very useful for what concerns the piezos, since their stroke dramatically reduces with decreasing of the temperature, and a better knowledge of their operating temperature greatly helps in the choice of the best device to be used as actuator.

| T sens | Cooldown value - K | Typical range during tests – K |
|---|---|---|
| **Piezo support** | 30 | 30-32 |
| **BT outer ring** | 20 | 20-22 |
| **Stepper motor** | 30 | 30-55 |

Table 16: Operating temperature of piezo frames and stepper motor during the Blade Tuner tests, inside HoBiCaT.

### 7.2.1. *STATIC TUNING RANGE TEST*

The full Blade Tuner frequency range has been measured using the cavity closed in PLL loop to track cavity frequency displacement. It took 205000 motor steps, corresponding to 10 complete turns of the CuBe screw, to cover the desired tuning range of about 520 kHz, where the frequency range has been kept this value to have a direct comparison with the former test inside CHECHIA. The measure has been repeated three times, although the last time we have stopped at one half of the trip backward (100000 steps) to perform the short range measurements. The full tuning range measurements are summarized in Fig. 51, while the corresponding tuning sensitivity is shown in Fig. 52.

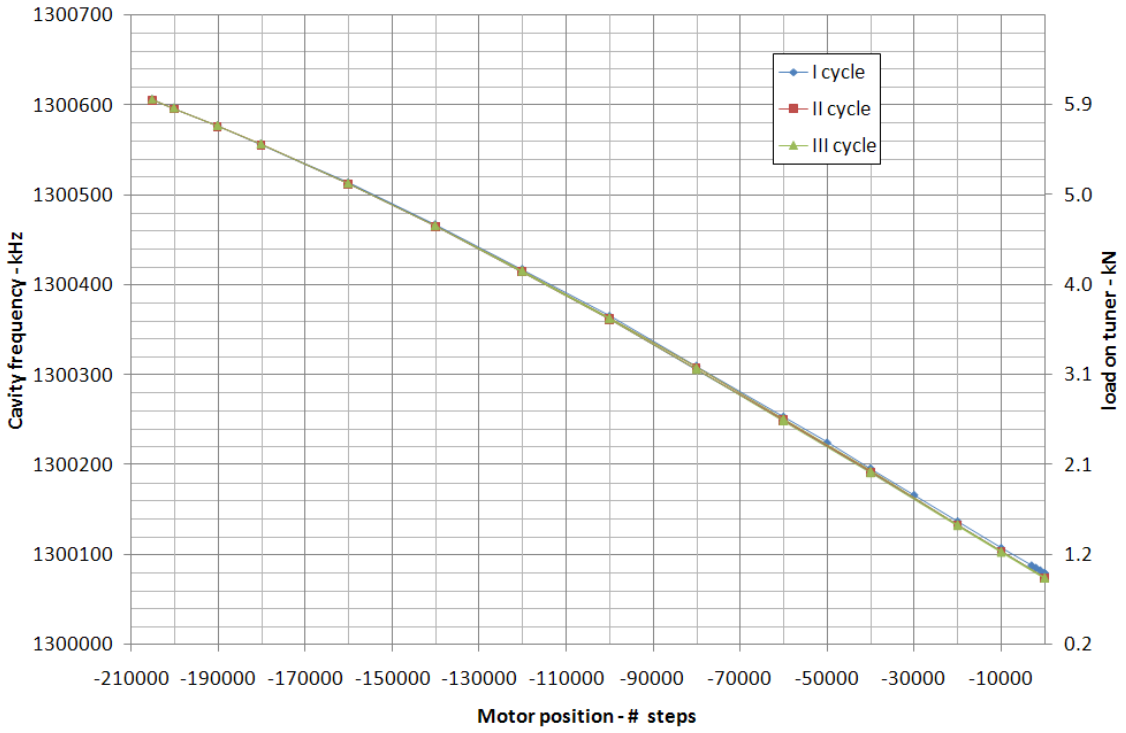


Fig. 51 – Tuning range vs. motor position curve

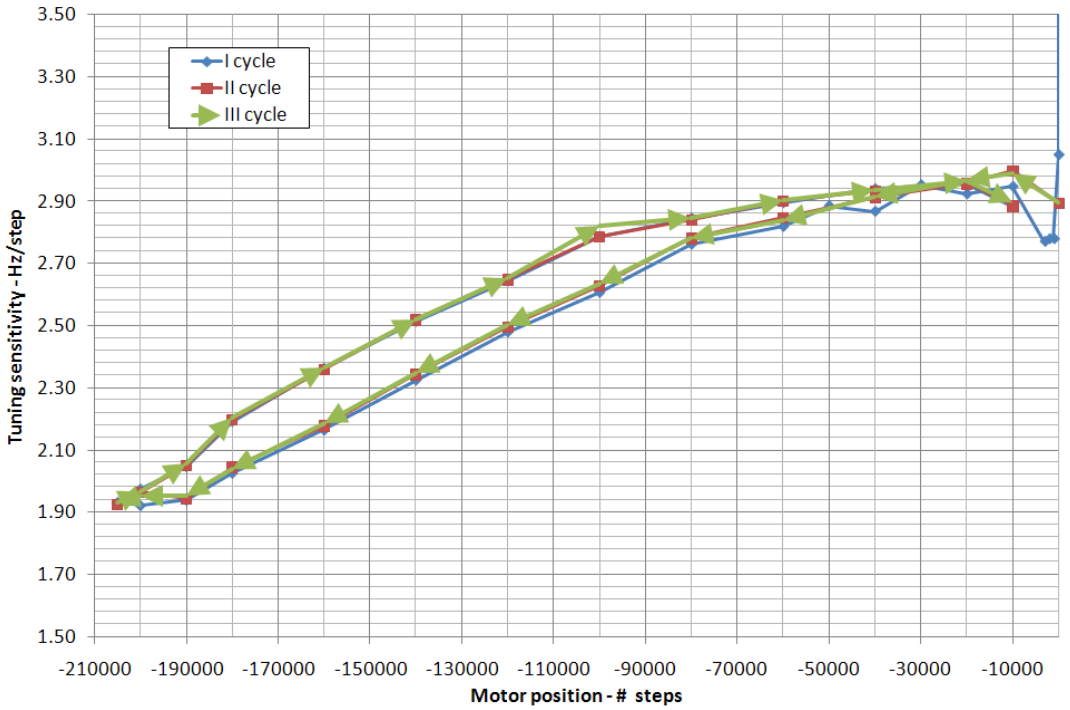


Fig. 52 – Tuning sensitivity vs. motor position

Fig. 53 shows a direct comparison between the performed tuning range at BESSY and DESY tests.

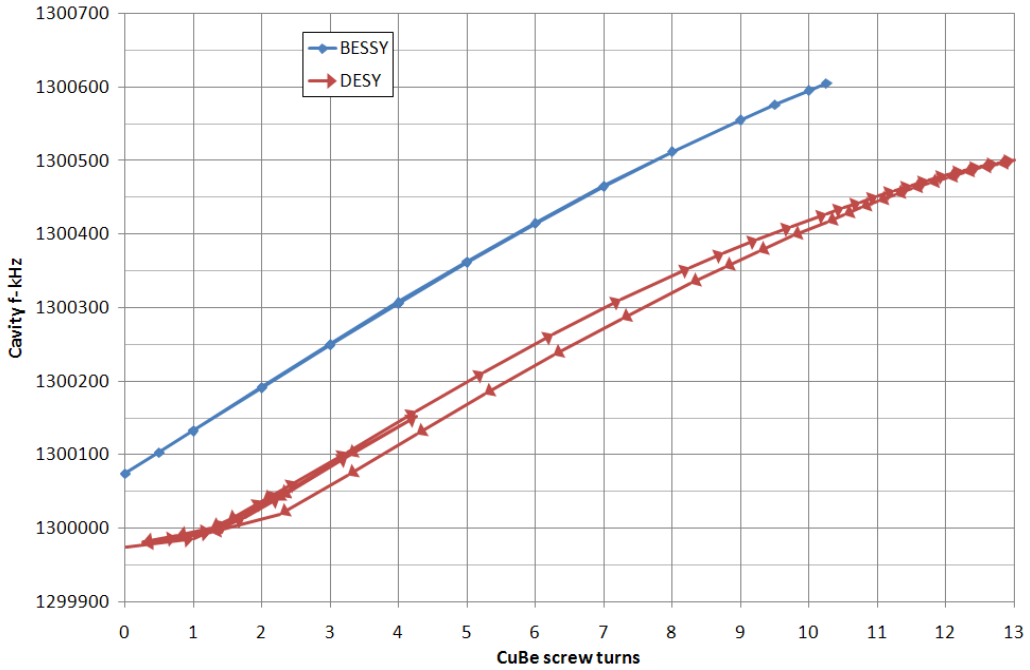


Fig. 53 – Comparison between the two graphs taken during thr tuning range tests inside CHECHIA and HoBiCaT. The reduction of the curve hysteresis is evident.

Table 16 collects the parameters of interest in evaluating the full tuning range results.

| | **BESSY** | **DESY** | **unit** |
|---|---|---|---|
| **Motor** | Phytron, 200 coils | Sanyo, 200 coils | |
| **Gear** | Phytron, VGPL, 100:1 | HD, 88:1 | |
| **Tuning range (TR)** | 525 | 520 | kHz |
| **CuBe screw turns** | 10.2 | 13 | # turns |
| **Motor full-steps** | -205000 | -228800 | # steps |
| **Max Δf over TR** | 1.7 (@-100000 steps) | 31 (@-79200 steps) | kHz |
| **Δf after full TR cycle** | 0.38 | 16 | kHz |
| **Max tuning sensitivity** | 3.0 | 1.6 x 2 | Hz/step |
| **Max load on tuner** | 6 | 5 | kN |

Table 16 – Stepper motor characteristics and summary of the tuning range results for the two different Blade Tuner tests

The full tuning range meets expectations and the large hysteresis measured at DESY has been significantly lowered after the 2$^{nd}$ cycle and even more lowered after the 3$^{rd}$ one. The 4$^{th}$ cycle was almost identical to the former one, meaning that all mechanical settlements were over.

Before concluding the 3$^{rd}$ complete tuning range cycle we stopped at -100000 steps position, chosen as the working point with the highest hysteresis width, and we performed different short tuning range measurements. In order to have a direct comparison to other TTF type I and II tuners data measured at BESSY, we performed both a measurement with the same motor step range (+/- 1000) and with the same frequency range (+/- 150 Hz, about +/- 60 steps). Fig. 54 shows the results of the first case, several complete cycles have been performed and the last measurements (made up by two complete cycles) are highlighted in both plots. Arrows show the direction kept during the test performance.

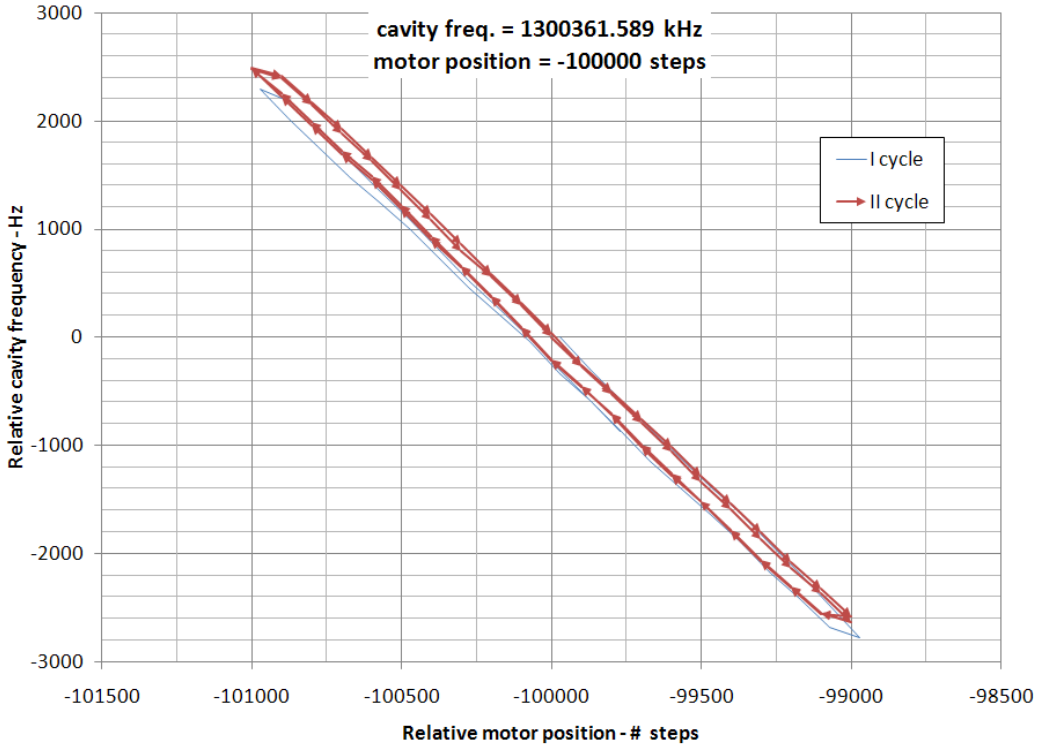


Fig. 54 – Short range tuning test

The assembly behaves as expected for what concerns the +/- 1000 steps curves. A backlash like effect is visible at both edges of the curve in Fig. 54, and the overall result, frequency offset Δf of about 0.2 kHz (over a tuning range of 5 kHz) and about 100 steps required, are comparable with the behavior of the TTF I tuner. A comparison between similar short range data between Blade Tuner and TTF I tuner is given in Table 17 [21] [22]. To help making a comparison between the different device performances, we have defined a parameter called "hysteresis factor" (of the small range curve) that is defined for both data set as:

$$hysteresis\ factor = 100 \cdot \frac{frequency\ range}{\Delta f}$$

| | **Blade Tuner** | **TTF I** | **Units** |
|---|---|---|---|
| Tuning sensitivity at the working point | 2.6 | 0.18 | HZ/step |
| Driving unit | Phytron VSS-UHVC 52.500 2.5 A GPL052-3UHVC/100:1 VGPL | Sanyo-Denki XS-735-010 HD 14-1010540 88:1 harmonic drive | Motor Gear |
| Steps range | +/- 1000 | +/- 1000 | # steps |
| cavity frequency range | 5100 | 330 | Hz |
| Δ frequency | 230 | 330 | Hz |
| Coercitive steps | < 100 | ~ 180 | # steps |
| "form factor" | 4.5 | 9 | % |

Table 17 – Short tuning range performances for TTF I and Blade Tuners.

Apart from the different tuning sensitivity in the working point of the two tuners, the two curves actually exhibit similar behavior and backlash level. The short tuning range in the

middle of the tuner range also meets the expectations when performing +/- 1000 motor steps over about +/- 2.5 kHz. Backlash-like effect is visible but well within the previous experiences with TTF I tuners.

### 7.2.2. *TESTS ON PIEZOS*

The cavity frequency displacement as induced by a DC driving voltage applied to piezo actuators was firstly measured using the closed PLL loop to track cavity frequency. Measurements were repeated for Piezo 1 alone, installed on motor side of the tuner, Piezo 2 alone as well as for Piezo 1 and 2 (1+2) in parallel. The piezo driving voltage was provided, for almost all measurements, by a Physics Instrumente (PI) piezo amplifier capable of +150 V maximum driving voltage. One last measure was performed using a PiezoMechanik amplifier designed for high voltage piezo (1000 V max voltage) in order to acquire a DC displacement curve for both piezo operated at the maximum nominal voltage of +200 V (for NOLIAC piezo

The typical hysteresis of this kind of PZT ceramic actuator can be also observed as expected. First curves were acquired with the tuner set at the lower end of the tuning range, corresponding to 0 steps. Then, the stepper motor has been moved to -40000 steps position. This corresponds to an overall compressive load on the tuner of about 2 kN and let us evaluating the difference in piezo stroke and hysteresis as a function of the load. Correspondent data are plotted in Fig. 55.

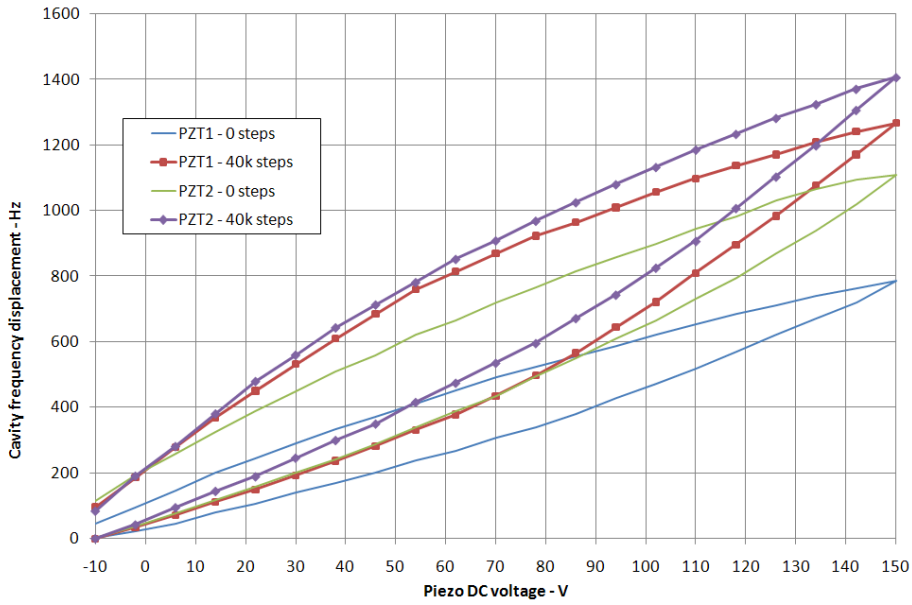


Fig. 55 – Piezo displacement vs. DC driving voltage

This analysis allows to evaluate also the different efficiency of the two piezos in transferring their stroke to the cavity, the final numerical results about this expected issue are reported in Table 18. Finally, both piezo 1 and 2 were operated in parallel with a DC driving voltage. The results, in terms of cavity frequency displacement, are shown in Fig. 56 for both +150 V and +200 V maximum driving voltage values.

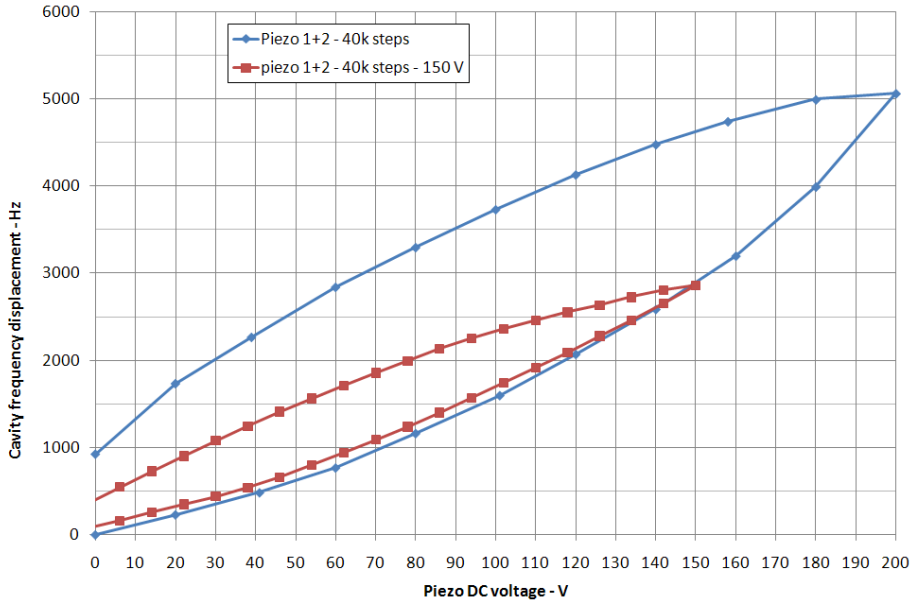


Fig. 56 – Piezo displacement when both piezos are driven together with a DC voltage

The numerical results from the performed DC piezo performance measurements are reported in Table 18. Values in *Italics* refer to theoretical results extrapolated by the measured ones assuming the same displacement ratio between piezo 1 and 2.

| **Motor position / total load** [# steps] / [kN] | **Voltage range** [V] | **Cavity Δf Piezo 1** (motor side) [kHz] | **Cavity Δf Piezo 2** [kHz] | **Cavity Δf Piezo 1+2** [kHz] | **Piezo 1&Piezo 2 Δf contribution** [%] |
|---|---|---|---|---|---|
| 0 / 1 | 0 - 150 | 0.79 | 1.11 | *1.9* | 42/58 |
| - 40000 / 2 | 0 – 150 | 1.27 | 1.41 | 2.86 | 47/53 |
| - 40000 / 2 | 0 -- 200 | *2.38* | *2.68* | 5.06 | *47/53* |

Table 18 – Summary of DC piezo performances

Results resumed in Table 18 confirm that:

- the frequency displacement induced by both piezos increased with the increasing load on the tuner (moving from 0 to -40000 steps), as expected by the improved mechanical coupling between actuators and cavity as well as by the slight stroke boost of PZT ceramic with pre-load.
- there is a minimum discrepancy between efficiency and coupling to cavity of the two piezos, but this discrepancy seemed to lower when moving to higher load.
- the use of both piezos in parallel actually results in a cavity static frequency shift that equals the sum of the two piezos independently.
- there is a significantly large margin in terms of detuning compensation performance with this piezos since more than 5 kHz max static shift have been measured. Since the static to dynamic performance ratio with the typical TTF pulse is assumed as close to 2 (also according to the ratio between the static and the dynamic Lorentz force coefficient), so high gradient pulsed operations Lorentz force detuning can be compensated even with current tuner assembly.

### 7.2.3. *TRANSFER FUNCTIONS*

Very accurate "piezo-to-RF" transfer functions have been acquired during overnight measurements (actually more than 9 hours of acquisition with a sensitivity less than 0.02 Hz), with the cavity resonance locked by the PLL. A SRS Lock-In Amplifier was used to excite the chosen piezo actuator and to read the phase detector output. The driving signal was sweeping from 5 Hz to 500 Hz, while the FM gain of the synthesizer used as a VCO (2000 Hz/V) is used to convert the PLL error signal to frequency shift. The resulting plots for amplitude and phase data are presented in Fig. 57.

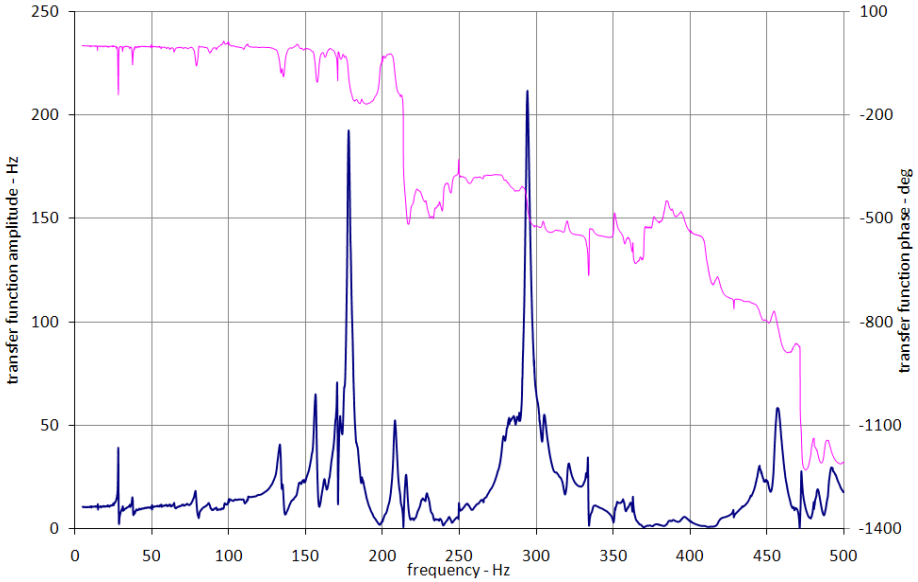


Fig. 57 – Transfer function between Piezo excitation and cavity detuning

Looking to the transfer functions one can say that the distribution and absolute amplitude of main modes are in agreement with usual experience on TTF cavity. In particular the sharp resonance at 30 Hz (key resonance for BESSY CW operations) is always present and corresponds to the lower cavity bending mode while peaks in the range 150 – 300 Hz correspond to main longitudinal compressive modes. Moreover the DC gain value as shown by the amplitude of the transfer function, about 10.5 Hz/V, matches the slope of the corresponding curve in Fig. 56 in the 10 V position (about 10 Hz/V). Finally, the slope of the transfer function phase curve at very low frequencies allows to estimate the assembly group delay. The results is 0.66 ms (considering phase data from 5 to 10 Hz), a value that is consistent with the delay that we had to apply to the driving pulses for the piezos during the LFD detuning compensation in the previous pulsed test at CHECHIA.

### 7.2.4. *MICROPHONICS*

Microphonics [21] spectra have been acquired several times for different position of the stepper motor. The reference analysis for the BESSY CW operations is the microphonics integrated power spectrum in the range $10^{-2}$ Hz to $10^{3}$ Hz. As a first result the values measured for the Z86 cavity equipped with Blade Tuner are consistent with the typical values measured with TTF tuner (without active compensation), i.e. with an amplitude in the order of 3 $Hz_{rms}$ with a major contribution from the 30 Hz resonance (two close resonances actually, due to a broken degeneracy of the vertical and horizontal bending modes).

### 7.2.5. *STATIC LORENTZ FORCE DETUNING COEFFICIENT*

The static Lorenz force detuning coefficient has also been measured. The test was anyway affected by several difficulties and probably by a large error, also due to the limited accelerating gradient that was achieved during the tests (about 8 MV/m of maximum accelerating field), this limitations mainly caused by multipactoring at the coupler site. The results are shown in Fig. 58. Linear interpolation reveals a static Lorentz coefficient close to to -1 Hz/(MV/m)$^2$ as expected by TESLA cavity design constraints.

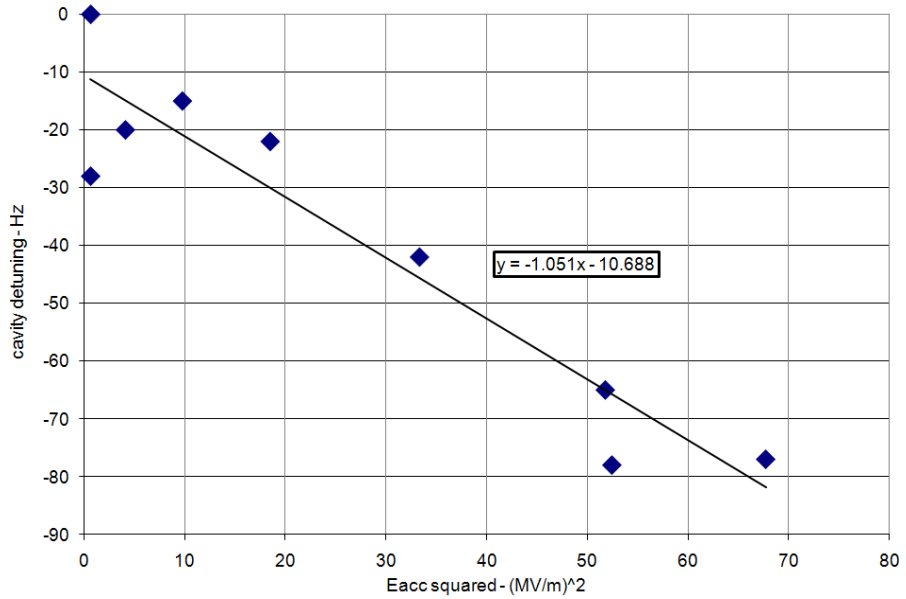


Fig. 58 –Cavity detuning vs. $E_{acc}^2$. The slope of the interpolating line is the the static Lorentz force detuning coefficient.

# 8. Evaluation of tuner operation

After the cold tests inside CHECHIA and HoBiCaT facilities, it is possible to say that coaxial Blade Tuner has successfully passed the prototype test. Every tuner component went through two complete cool-down and warm-up procedures, comprehensive of assembling and disassembling in different facilities, without damages or failures. More than 520 kHz of tuning range has been achieved in each facility, with margin left to push even to higher tuning capabilities. The non negligible hysteresis of the first test inside CHECHIA has been greatly reduced starting from the second test cycle inside HoBiCaT, passing from the former frequency error after a full tuning range cycle of 16 kHz to the current at regime maximum frequency uncertainty of 380 Hz over a full frequency span. Moreover short range tests has shown that the uncertainty is due to the driving system backlash, and the actual value can be reduced changing the frequency sensitivity via the demultiplication apparatus if needed. Pulsed tests inside CHECHIA has shown that the entire LFD shown by Z86 cavity at the maximum reached gradient of 23 MV/m has been compensated in different load conditions and with each possible piezo configuration, while the CW tests inside HoBiCat has revealed a static Lorentz coefficient close to to -1 Hz/(MV/m)$^2$, as expected by TESLA cavity design constraints. Finally, testing in CW the tuning capability of the piezos inside HoBiCat, a static frequency shift superior to 5 kHz if the piezo are operated in parallel at 200 V driving voltage has been measured. This corresponds to about 2.5 kHz frequency shift in dynamic regime,

and so assuring great margin for the compensation of the expected LFD at 35 MV/m of about 1 kHz for ILC cavities.

During the CHECHIA test, a LFD value higher than expected for the achieved gradient has been found. This is probably due to the limited axial stiffness of the old He tank used. With the final Slim Blade tuner Helium tank design, see Fig. 59, it is expected to restore or even lower the usual Lorentz force sensitivity.

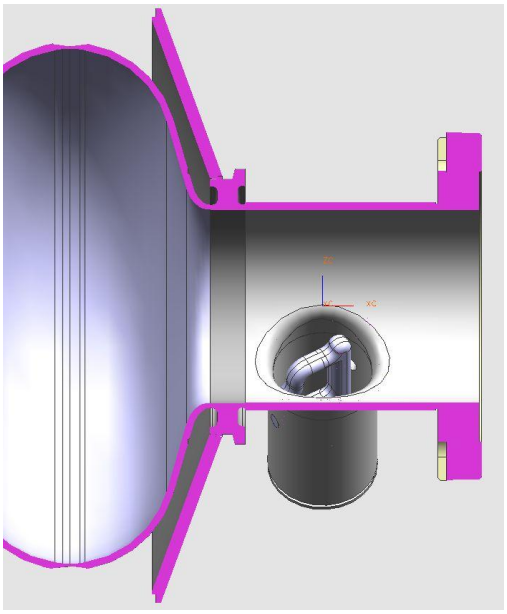

Fig. 59 – 3D view of the proposed solution for the revised end group

Finally, the present stage of coaxial tuner development, equipped with the cheaper piezo option, 40 mm stacks instead of 70 mm previously foreseen, can be considered partially fulfilling XFEL requirements [25], but the needed modifications toward this goal are on the way. These modifications can be summarized in these three points:

- Blade re-distribution over the tuner circumference. The 4-blades pack that is closer to each piezo position is doubled so that two packs in parallel bear the compressive load exerted on the tuner through each actuator. The overall number of blades is anyway even lowered using 3-blads packs for the remaining position over the tuner circumference (92 vs. 96 blades of the previous design revision) and the blade design is also preserved. This redistribution will modulate the stiffness of the tuner ring so that it is maximized exactly where the forces are applied (piezo sites). This leads to a higher overall longitudinal stiffness for the installed Blade Tuner.
- Different assembly angle. It has been chosen to increase the clearance between the Blade Tuner and the gas return pipe (GRP) of the cryomodule. This new layout also slightly, but favorably, changes the piezo position from the edge of the half-ring toward its center.
- Priority to the titanium material option. Lighter and compatible with Nb in terms of thermal shrinkage coefficients, thus completely eliminating the problem of excessive cavity deformation during cooldown. Anyway the experience gained with Slim_SS and Slim_Ti tests led to the choice of an increased blade thickness compared to previous design, from 0.5 to 0.8 mm, in order to gain higher clearance from the buckling region.

These modifications are shown in Fig. 60.

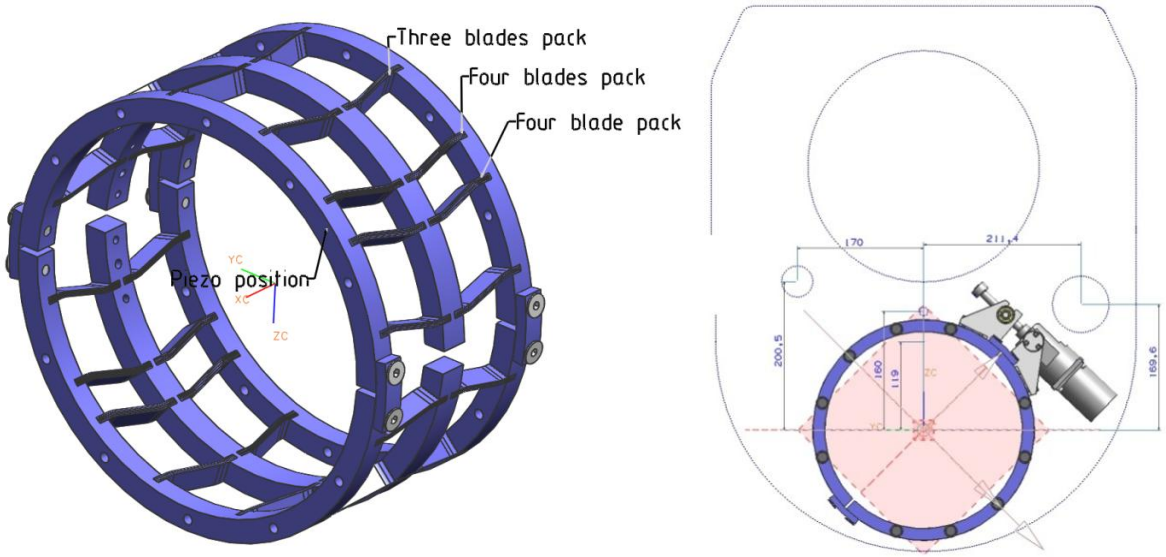


Fig. 60 – The final Blade Tuner design (left) and its revised positioning inside the cryomodule

We are confident that, when these modifications will be done, the final tuner configuration, coupled to the final He tank, will fulfill the even more severe specifications foreseen for ILC.

## Acknowledgements

Many thanks go to the people of DESY and BESSY labs with whom we performed our tuner evaluation tests, for letting us use their facilities and having shared with us their great expertise, and their infinite kindness hosting us for long time measurements.

Also, we acknowledge the support of the European Community-Research Infrastructure Activity under the FP6 “Structuring the European Research Area” programme (CARE, contract number RII3-CT-2003-506395).

Last but not least, a big thank you is also directed to our French, German and Polish colleagues that, inside the CARE SRF WP8 working group, have helped us realizing our goals with kind collaboration and useful discussions.

## References

[1] TESLA Technical Design Report. Part II: The Accelerator TESLA, 2001. (http://tesla.desy.de/new_pages/TDR_CD/PartII/accel.html)

[2] H.Kaiser. New approaches to tuning of TESLA resonators. Proceedings of 9th Workshop on RFSC. Santa Fe, US : s.n., 1999.

[3] J. Sekutowicz, M. Ferrario, Ch. Tang. Superconducting superstructure for the TESLA collider: A concept. PHYSICAL REVIEW SPECIAL TOPICS - ACCELERATORS AND BEAMS, VOLUME 2, 062001. 1999.

[4] C.Pagani, A.Bosotti, P.Michelato, R.Paparella, N.Panzeri, P.Pierini, F.Puricelli, G.Corniani. Report on Fast Piezo Blade Tuner (UMI Tuner) for SCRF Resonators Design and Fabrication. CARE note-2005-21-SRF. 2005.

[5] Bathe, K.J. Finite Element Procedures. : Prentice Hall, 1996.

[6] P. Sekalski, A. Napieralski DMCS Technical University of Lodz, S. Simrock, L. Lilje DESY, A. Bosotti, R. Paparella, F. Puricelli INFN Milan, M. Fouaidy IN2P3 ORSAY, Static Absolute Force Measurement for Preloaded Piezoelements Used for Active Lorentz Force Detuning System, Proceedings of LINAC 2004, Lübeck Germany.

[7] A. Bosotti, R. Paparella, F. Puricelli. Extreme piezo lifetime test report. : Physick Intrumente technical notes, 2005.

[8] A. Bosotti, P. Pierini, P. Michelato, C. Pagani, R. Paparella, N. Panzeri, L. Monaco,R. Paulon, M. Novati, CARE activities on superconducting RF cavities at INFN Milano (Invited Talk), proceedings SPIE 05, Warsaw 28 August – 2 September 2005.

[9] M. Liepe, W.D.-Moeller, S.N. Simrock, "Dynamic Lorentz Force Compensation with a Fast Piezoelectric Tuner", Proceedings of the 2001 Particle Accelerator Conference, Chicago, p. 1074-1076

[10] D. Barni, A. Bosotti, C. Pagani, R. Lange, H.B. Peters, "A new tuner for Tesla", Proceedings of EPAC 2002, Paris, France, 2205-2207

[11] F. Puricelli, "Attuatori piezoelettrici in ambiente criogenico per il controllo di strutture acceleranti avanzate", Master Thesis, 2005, University of Milan, Milan.

[12] Paparella, Rocco. Fast Frequency Tuner for high gradient SC cavities for ILC and XFEL. Ph D Thesis. INFN Milano : Università degli Studi di Milano, 2008.

[13] W.D.Moeller, B.Petersen, B.Sparr A Proposal for a TESLA Accelerator Module Test Facility, TESLA Report No. 2001-08

[14] P. Sekalski, A. Napieralski, Technical University of Lodz, Poland , S. Simrock, C. Albrecht, L. Lilje , DESY, Hamburg, Germany ,P. Bosland, CEA, Sacley, France , M. Fouaidy, IPN, Orsay, France , A. Bosotti, INFN, Milan, Italy, Smart Materials Based System Operated at 2K Used as a Superconducting Cavity Tuner for VUV-FEL Purpose, Proceedings of 10th International Conference on New Actuators, Bremen (Germany), 14-16 June 2006.

[15] Tariq, Salman. 1.3GHz Cavity/Cryostat Stiffness Model & Tuning Sensitivity. SRF Engineering Meeting, 15/2/2006. Batavia, US : FNAL, 2006.

[16] C. Pagani, A. Bosotti, P. Michelato, N. Panzeri, R. Paparella, P. Pierini. ILC Coaxial Blade Tuner. Proceedings of EPAC06. Edinburgh, UK : s.n., 2006.

[17] R.Hill. The Mathematical Theory of Plasticity. Oxford : Clarendon Press, 1950.

[18] C. Pagani, A. Bosotti, N. Panzeri. Improved design of the ILC Blade-Tuner for large scale production. Proceedings of PAC07. Albuquerque, US : s.n., 2007.

[19] Lutz Lilje XFEL: Plans for 101 Cryomodules, proceedings of SRF 2007, Peking University, Beijing, China,

[20] J. Knobloch, W. Anders, D. Pflückhahn, and M. Schuster, A Test Facility For Superconducting RF Systems, SRF2003

[21] Oliver Kugeler , Wolfgang Anders, Jens Knobloch, Axel Neumann, Microphonics Measurements in a CW-driven TESLA-type Cavity MOPCH149, Proceedings of EPAC 2006, Edinburgh, Scotland

[22] O. Kugeler, Measurement and compensation of microphonics in CW operated TESLA-type cavities, ERL07, Daresbury Laboratory, UK, May 21-25, 2007.

[23] P. Sekalski et al., "Static Absolute Force Measurement for Preloaded Piezoelements used for Fast Lorentz Force Detuning System", in Proceedings of Linac 2004, Lubeck, Germany, p. 486.

[24] C. Pagani, A. Bosotti, N. Panzeri, R. Paparella, P. Pierini, INFN Milano, Italy, C. Albrecht, R. Lange, L. Lilje, DESY Hamburg, Germany, Piezo-Assisted Blade Tuner Cold Test Results, proceedings of SRF 2007, Peking University, Beijing, China,

[25] The Technical Design Report of the European XFEL (http://xfel.desy.de/localfsExplorer_read?currentPath=/afs/desy.de/group/xfel/wof/EPT/TDR/XFEL-TDR-final.pdf)

[26] ILC Design report – Volume 3 – The Accelerator (http://ilcdoc.linearcollider.org/getfile.py?docid=182&name=ILC_RDR_Volume_3-Accelerator&format=pdf)

[27] P. Sekalski, "Smart Materials as Sensors and Actuators for Lorentz Force Tuning System", Ph.D thesis, 2007, Technical University of Łódź, Poland.

# APPENDIX

| Manufactures | | Noliac | Noliac | Epcos | PI | Noliac | Piezomechanik |
|---|---|---|---|---|---|---|---|
| Model | | SCMA/S1/A/10/10 /40/200/60/4000 | SCMA/S2/A/15/15 /70/200/100/9000 | LN 01/8002 | P-888.90 | SCMAS/S1/A/10/10 /30/200/42/6000 | Pst 150/10 |
| Referred as | | NOLIAC_40 | NOLIAC_70 | EPCOS_30 | PI_36 | NOLIAC_30 | PM |
| Material | | medium soft doped PZT-S1 | medium soft doped PZT-S2 | PZT-nd34 | PZT-PIC 255 | medium soft doped PZT-S1 | |
| Case preload | | No | no | no | no | no | Yes / 400N |
| Length | mm | 40 ± 0,5 | 70 ± 0,8 | 30 | 36 | 30 ± 0,5 | 64 |
| Active length | mm | | 68.5 | | 33.84 | | |
| Cross section | mm x mm | (10 x 10) ± 0,2 | (15 x 15) ± 0,3 | 6,8 x 6,8 | 10 x 10 | (10 x 10) ± 0,2 | |
| Number of layers | | | 490 | | 300 | 196 | |
| Average layer thickness | µm | | 140 | | 113 | 140 | |
| Young modulus | kN/mm² | 45 | 47 | 51 | 48.3 | 45 | |
| Stiffness: small range bulk | kN/mm | 67 / 112 | 90 / 151 | 80 / 83 | 103 / 105 | 95 / 150 | 25 / 35 |
| Max. stroke | µm | 60 ± 9 | 100 ± 13 | 40 | 35 ± 3,5 | 42 ± 6,3 | 80 |
| Blocking Force | N | 4000 ± 800 | 9000 ± 1400 | 3200 | 3600 ± 720 | 4000 ± 800 | |
| Load Limit | N | 12000 | 27000 | | 10000 | | |
| Resonant freq. no load | kHz | 38 | | 52 | 40 | 51 | |
| Density | kg/m³ | 7,7 10³ | 7,5 10³ | 7,75 10³ | 7,8 10³ | 7,7 10³ | |
| Min. voltage | | 0 | 0 | 0 | -20 | 0 | -30 |
| Max. voltage | V | 200 | 200 | 160 | 120 | 200 | 150 |
| Max speed - unloaded | V/µs | | | 1.6 | | | |
| Max. charge current | A | | | 20 | | | |
| Capacitance | µF | 8 | 40 | 2.1 | 12.4 | 5.7 | |
| Loss Factor | tan(ô) | 0.017 | | 0.019 | 0.015 | 0.017 | |
| Thermal Expansion | ppm/K | -2.5 | | | | -2.5 | |

Table 19 – Properties of piezos evaluated for possible use in the Blade Tuner.